Quantum Error Correction and Applications in Condensed Matter Physics

U.S. Quantum Information Science School, August 12, 2023, Fermi National Laboratory

Peter P. Orth (Ames National Laboratory and Saarland University)

Outline and Take-Home Messages

- Quantum Computing Applications to Condensed Matter Physics
  - Condensed Matter & Material Science provides a rich & relevant set of problems
    - Difficulty level is often tunable
    - Many classical computational approaches are known to compare to
    - Open question which problems are best suited to demonstrate quantum advantage
  - Hybrid quantum-classical simulations leverage both classical & quantum computing power
    - One example is the variational quantum eigensolver (VQE) (see tutorial yesterday)
  - Simulations of nonequilibrium dynamics are classically hard due to entanglement growth
    - Opportunity for quantum computing

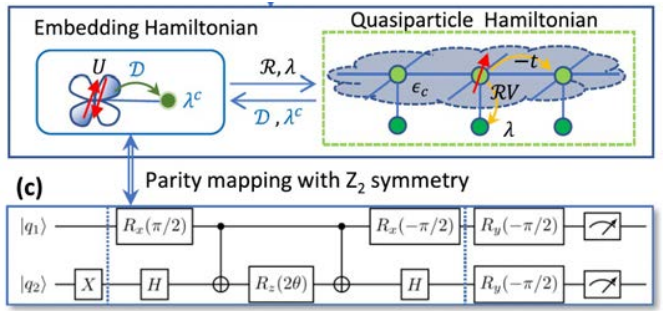

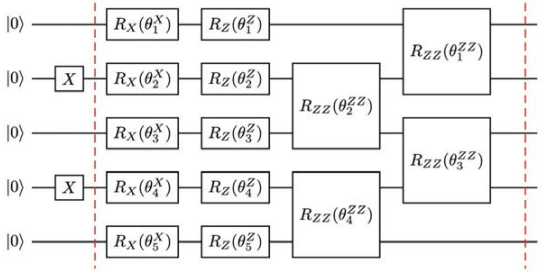

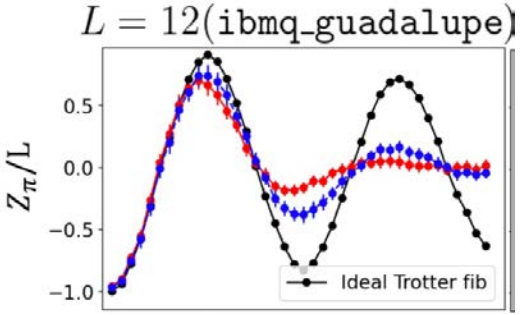

Outline and Take-Home Messages

- Quantum Computing Applications to Condensed Matter Physics
  - Condensed Matter & Material Science provides a rich & relevant set of problems
    - Difficulty level is often tunable
    - Many classical computational approaches are known to compare to
    - Open question which problems are best suited to demonstrate quantum advantage
  - Hybrid quantum-classical simulations leverage both classical & quantum computing power
    - One example is the variational quantum eigensolver (VQE) (see tutorial yesterday)
  - Simulations of nonequilibrium dynamics are classically hard due to entanglement growth
    - Opportunity for quantum computing
- Quantum Error Correction (QEC)
  - Primary goal of the field that is required to unlock the full potential of quantum computing
  - Main idea: Protect quantum memory from noise and perform fault-tolerant operations
  - Many flavors and QEC codes exist (e.g. QEC Zoo[1]): Here focus on the basic principles.

[1] www.quantumerrorcorrectionzoo.org

Quantum Error Correction: Basics

Motivation and repetition codes

- Errors in a quantum computation are unavoidable due to
  - Contact with environment ➢ leads to decoherence
  - Unitary gate set is continuous ➢ gate errors can be arbitrarily small $U = U_{\text{ideal}}[1 + \mathcal{O}(\epsilon)]$
- Quantum Error Correction (QEC) protects quantum information by adding redundant information
  - Same idea as in Classical Error Correction

Code distance

$$d = \min_{x,y \in C} D_H(x, y)$$

Errors of weight up to $\frac{d-1}{2}$ can be corrected

x	encoding →	y	noise →	$\tilde{y}$	decoding →	$\tilde{x}$
0		$(000) \in C$		$(001) \notin C$		0
1		$(111) \in C$		$(011) \notin C$		1
0		(000)		(011)		1

Singe bit flips can be corrected

Two bit flips result in logical error

Failure probability: $3p^2(1-p) + p^2 < p \Rightarrow p < 1/2$

Challenges for QEC

- Phase errors occur in addition to bit flip errors

$$|0\rangle \to |0\rangle$$
$$|1\rangle \to -|1\rangle$$

$$|+\rangle = \frac{1}{\sqrt{2}}[|0\rangle + |1\rangle \to \frac{1}{\sqrt{2}}[|0\rangle - |1\rangle] = |-\rangle$$

Phase flips act as bit flips of X eigenstates!

- Errors can be arbitrarily small and are continuous
- Measurement necessarily causes disturbance
  - Projective measurement projects onto eigenspace of measurement operator
- No cloning theorem (cannot copy quantum information)

3-qubit bit flip code

$$|0\rangle \to |\bar{0}\rangle = |000\rangle$$

$$|1\rangle \to |\bar{1}\rangle = |111\rangle$$

$$|\psi\rangle = a|0\rangle + b|1\rangle$$

Logical operators

$$X_L = X_1 X_2 X_3$$
$$Z_L = Z_1 Z_2 Z_3$$

Encoding circuit:

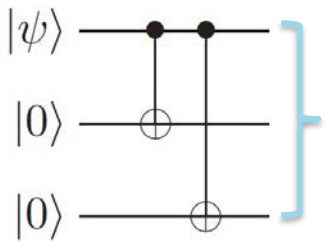

$$a|\bar{0}\rangle + b|\bar{1}\rangle$$

Protected against $\{X_1, X_2, X_3\}$ errors.

Bit flip code: error detection via syndrome measurement

- Measure Pauli strings (Z_1Z_2, Z_1Z_3) ☞ yields error syndrome $(\pm 1, \pm 1)$

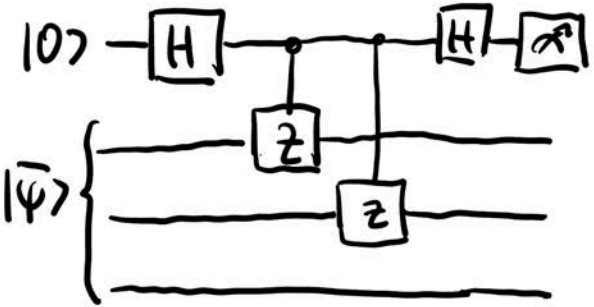

Z_1Z_2	Z_2Z_3	Error type	Action
$+1$	$+1$	no error	no action
$+1$	-1	bit 3 flipped	flip bit 3
-1	$+1$	bit 1 flipped	flip bit 1
-1	-1	bit 2 flipped	flip bit 2

by majority vote

$$|0\rangle|\bar{\psi}\rangle \to \frac{1}{\sqrt{2}}(|0\rangle + |1\rangle)|\bar{\psi}\rangle \to \frac{1}{\sqrt{2}}\Big(|0\rangle|\bar{\psi}\rangle + Z_1Z_2|1\rangle|\bar{\psi}\rangle\Big)$$

$$\to \frac{1}{2}\Big([|0\rangle + |1\rangle]|\bar{\psi}\rangle + Z_1Z_2[|0\rangle - |1\rangle]|\bar{\psi}\rangle\Big) = \frac{1}{2}\Big(1 + Z_1Z_2\Big)|0\rangle|\bar{\psi}\rangle + \frac{1}{2}\Big(1 - Z_1Z_2\Big)|1\rangle|\bar{\psi}\rangle$$

Measurement of ancilla collapses logical qubit to $\frac{I \pm Z_1Z_2}{2}$ orthogonal eigenspaces

⇒ Digitization of error: bit flip either occurs (with small probability) or not.

Orthogonal error subspaces

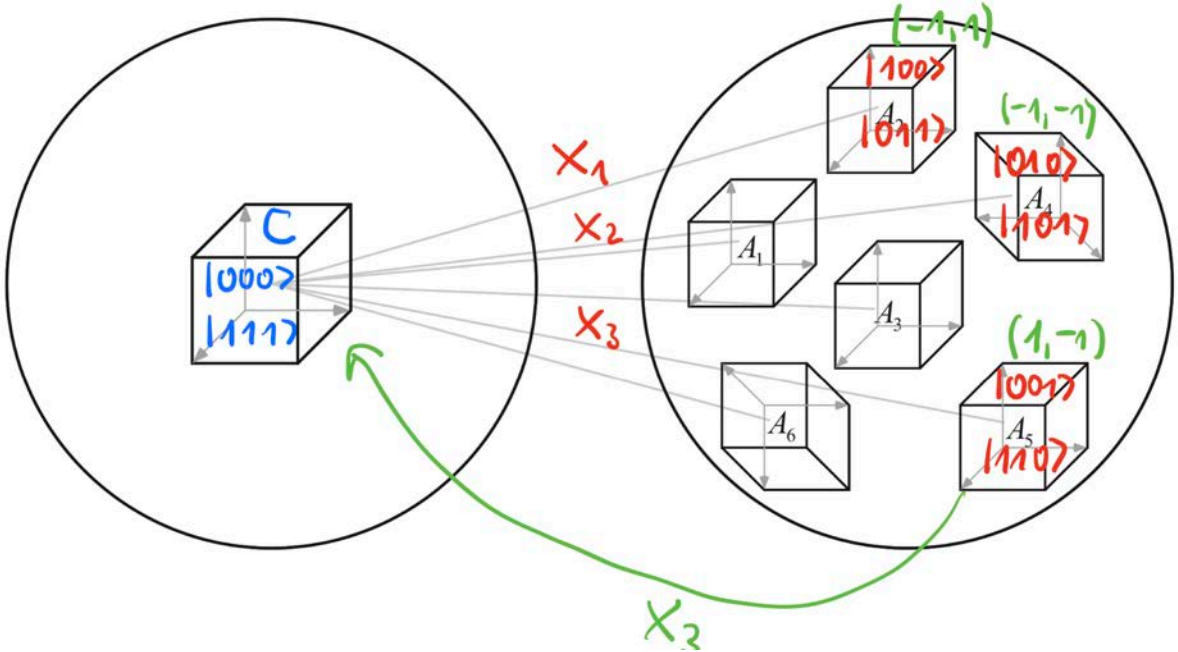

- Ancilla measurement discretizes error by projecting states onto orthogonal and undeformed error subspaces
- Recovery operation associated with each syndrome outcome $(\pm 1, \pm 1)$

Two and three bit flip errors are not correctable

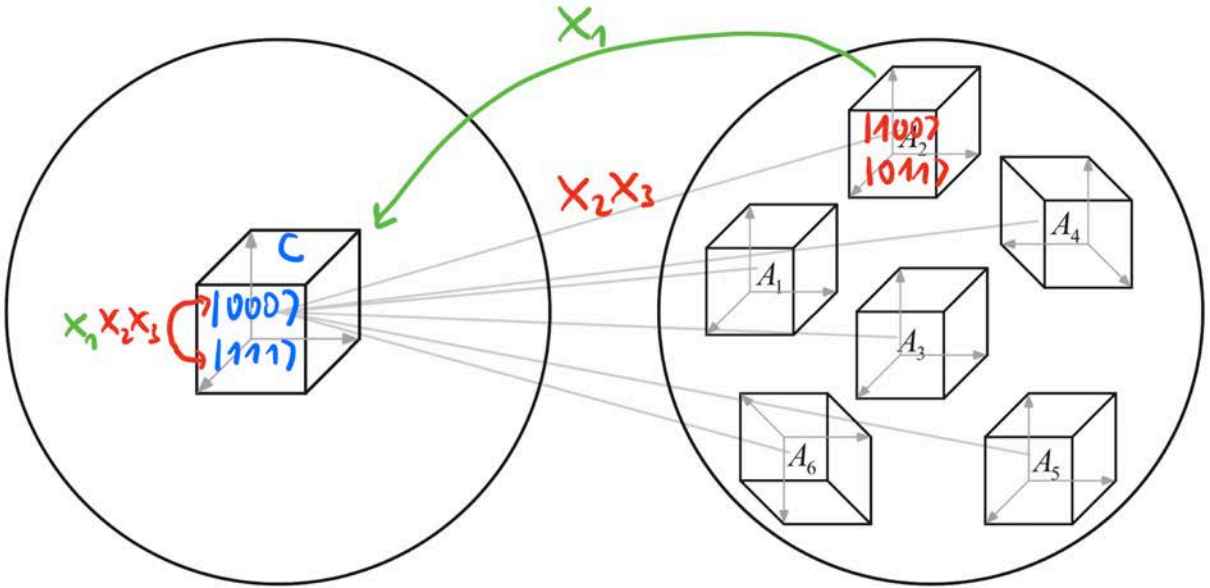

- Two-bit flip errors is erroneously corrected ☞ logical error
- Three-bit flip error correspond to logical operation and cannot be detected

Challenges for QEC: almost all addressed in bit flip code

- Phase errors occur in addition to bit flip errors ❌ (still need to be addressed)

$$|0\rangle \to |0\rangle \qquad |1\rangle \to -|1\rangle \quad \Rightarrow \quad |+\rangle = \frac{1}{\sqrt{2}}[|0\rangle + |1\rangle \to \frac{1}{\sqrt{2}}[|0\rangle - |1\rangle] = |-\rangle$$

Phase flips act as bit flips of X eigenstates!

- Errors can be arbitrarily small and are continuous
  - Ancilla measurement discretizes errors (either they occur or not) ✅
- Measurement necessarily causes disturbance
  - Projective measurement projects onto eigenspace of measurement operator
  - Measurement of syndrome operators does not affect information encoded in code subspace C ✅
  - Projection is actually a good thing ✅
- No cloning theorem (cannot copy quantum information)
  - We never copied the state $|\psi\rangle = a|0\rangle + b|1\rangle$ ✅

Phase flip code

- Phase errors occur in addition to bit flip errors ✅

$$|0\rangle \to |0\rangle$$
$$|1\rangle \to -|1\rangle$$

$$\Rightarrow \quad |+\rangle = \frac{1}{\sqrt{2}}[|0\rangle + |1\rangle \to \frac{1}{\sqrt{2}}[|0\rangle - |1\rangle] = |-\rangle$$

Phase flips act as bit flips of X eigenstates!

3-qubit phase flip code

$$|0\rangle \to |\bar{0}\rangle = |+++\rangle = \frac{1}{\sqrt{2}}(|0\rangle + |1\rangle)^{\otimes 3}$$

$$|1\rangle \to |\bar{1}\rangle = |---\rangle = \frac{1}{\sqrt{2}}(|0\rangle - |1\rangle)^{\otimes 3}$$

Protected against $\{Z_1, Z_2, Z_2\}$ errors.

Syndrome measurements

$$(X_1X_2, X_1X_3) = (\pm 1, \pm 1)$$

Encoding circuit:

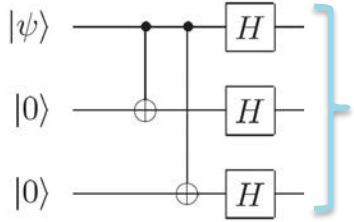

$$a|\bar{0}\rangle + b|\bar{1}\rangle$$

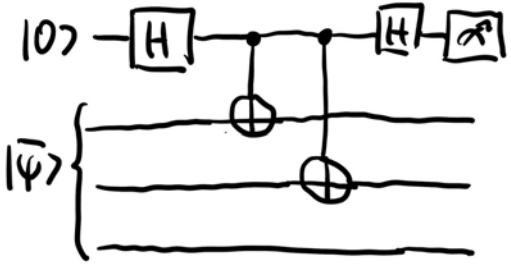

Circuit to measure

$$X_1X_2$$

Combine bit and phase flip code: Shor's 9-qubit code

- Shor's 9-qubit code protects against all single bit and phase flip errors and their combination
- Codewords

$$|0\rangle \to |\bar{0}\rangle = \frac{1}{2^{3/2}}(|000\rangle + |111\rangle)(|000\rangle + |111\rangle)(|000\rangle + |111\rangle)$$
$$|1\rangle \to |\bar{1}\rangle = \frac{1}{2^{3/2}}(|000\rangle - |111\rangle)(|000\rangle - |111\rangle)(|000\rangle - |111\rangle)$$

- Detect bit flips by syndrome measurements of $(Z_1Z_2, Z_1Z_3, Z_4Z_5, Z_4Z_6, Z_7Z_8, Z_7Z_9)$
- Detect phase flips by syndrome measurements $(X_1X_2X_3X_4X_5X_6, X_4X_5X_6X_7X_8X_9)$
- Information encoded nonlocally

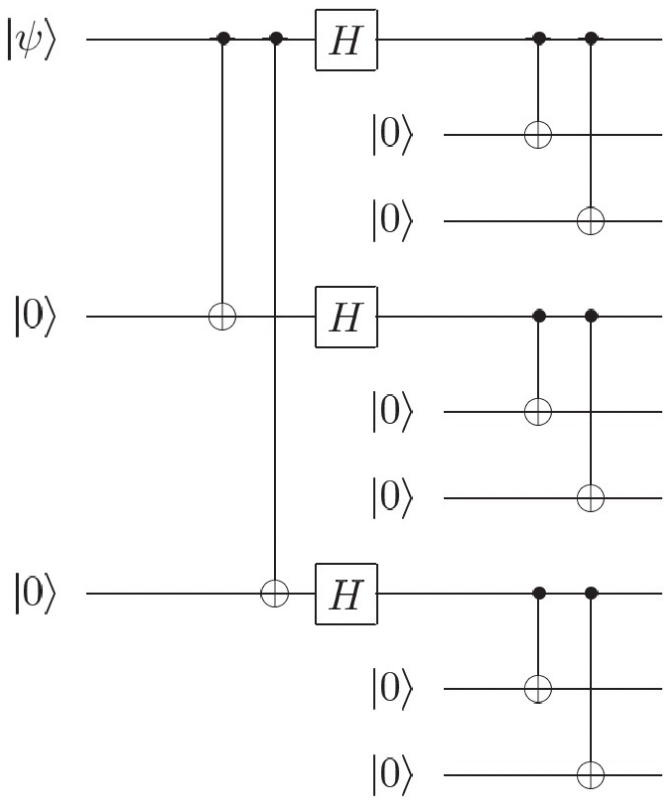

Code distance and uncorrectable errors

- Two bit flips in a single cluster of three qubits cannot be corrected (instead we incorrectly apply X_3)

$$X_3X_1X_2|\bar{0}\rangle = |\bar{0}\rangle$$
$$X_3X_1X_2|\bar{1}\rangle = -|\bar{1}\rangle$$

$$\Rightarrow \quad Z_L(a|\bar{0}\rangle + b|\bar{1}\rangle = a|\bar{0}\rangle - b|\bar{1}\rangle$$

results in a logical phase flip

- Two phase flips in different clusters cannot be corrected

$$Z_7Z_1Z_4|\bar{0}\rangle = |\bar{1}\rangle$$
$$Z_7Z_1Z_4|\bar{1}\rangle = |\bar{0}\rangle$$

$$\Rightarrow \quad X_L(a|\bar{0}\rangle + b|\bar{1}\rangle = a|\bar{1}\rangle + b|\bar{0}\rangle$$

results in a logical bit flip

- Only weight t=1 Pauli errors can be corrected ☞ Code distance $d = 2t + 1 = 3$

Are there two qubit errors that can be corrected?

- Shor's code is a $[[n, k, d]] = [[9, 1, 3]]$ code.

Error probability

- Unencoded qubit: failure with probability p
- Shor's logical qubit
  - Logical phase error requires two bits on the same cluster to flip
    - Upper bounded by

$$p_{L,\text{phase}} \leq 3\binom{3}{2}\left(\frac{2}{3}p\right)^2 = 4p^2$$

  - Logical bit flip error requires two bits on different clusters to undergo phase error
    - Upper bounded by

$$p_{L,\text{bit}} \leq \binom{3}{2}3^2\left(\frac{2}{3}p\right)^2 = 12p^2$$

  - Encoding is advantageous for

$$\boxed{p_{L,\text{tot}} = 16p^2 \leq p^2 \Rightarrow p < 1/16}$$

- Encoded qubit has smaller failure rate for small enough physical failure rate

Conditions for Quantum Error Correction

- Define set of correctable errors $\mathcal{E} \subseteq \mathcal{P}_n = \{I, X, Y, Z\}^{\otimes n}$
  - Typical example: all Pauli errors of weight $\leq t$
- Starting from any state $|\bar{i}\rangle \in C$, wish to undo any action composed of errors in $\mathcal{E}$

Error map (Stinespring dilation representation):

$$|\bar{i}\rangle|0\rangle_E \to \sum_\mu M_\mu |\bar{i}\rangle|\mu\rangle_E$$

Error entangles system with environment!

orthonormal states

Kraus operators $M_\mu = \sum_a c_{\mu a} P_a$

- Can reverse errors if there exists a recovery superoperator defined via $\{R_\nu\}$ such that

$$\sum_{\nu,\mu} R_\nu M_\mu |\bar{i}\rangle|\mu\rangle_E|\nu\rangle_A = |\bar{i}\rangle|\text{stuff}\rangle_{EA}$$

$$R_\nu M_\mu |\bar{i}\rangle = \lambda_{\nu\mu}|\bar{i}\rangle$$

- Entanglement has been shifted to occur between environment & ancillas
- State $|\text{stuff}\rangle_{EA}$ must not depend on i
- $R_\nu M_\mu$ acts as identity on codespace C

Conditions for Quantum Error Correction

- Using completeness condition $\sum_\nu R_\nu^\dagger R_\nu = I$, we find

$$M_\delta^\dagger M_\mu |\bar{i}\rangle = M_\delta^\dagger (\sum_\nu R_\nu^\dagger R_\nu) M_\mu |\bar{i}\rangle = \sum_\nu \lambda_{\nu\delta}^* \lambda_{\nu\mu} |\bar{i}\rangle$$

Also acts as identity on codespace C

$$R_\nu M_\mu |\bar{i}\rangle = \lambda_{\nu\mu} |\bar{i}\rangle$$

- Necessary and sufficient condition on codespace C for allowing errors in $\mathcal{E}$ to be corrected is

$$\boxed{\langle \bar{j} | M_\delta^\dagger M_\mu | \bar{i}\rangle = C_{\delta\mu}\delta_{ij}}$$

Arbitrary Hermitian matrix that is independent of i,j

Since $M_\mu = \sum_a c_{\mu a} P_a$

this implies

$$\boxed{\langle \bar{j} | P_b P_a | \bar{i}\rangle = C_{ba}\delta_{ij} \text{ for } P_a, P_b \in \mathcal{E}}$$

Alternative derivation of QEC condition

- Consider the code block is in any state $|\bar{\psi}\rangle$ and then an error acts:

$$|\bar{\psi}\rangle|0\rangle_E \to \sum_\mu M_\mu|\bar{\psi}\rangle|\mu\rangle_E$$

- The reduced density matrix of the environment must not carry any information about the state $|\bar{\psi}\rangle$

$$\rho_E = \sum_{\mu,\nu} |\mu\rangle_E \langle\bar{\psi}|M_\nu^\dagger M_\mu|\bar{\psi}\rangle\langle\nu|_E$$

Must be independent of $|\bar{\psi}\rangle = \sum_i c_i|\bar{i}\rangle$

$$\rho_E = \sum_{i,j}\sum_{\mu,\nu} c_i^* c_j |\mu\rangle_E \langle\bar{i}|M_\nu^\dagger M_\mu|\bar{j}\rangle\langle\nu|_E$$

Independence from c_i implies that $\boxed{\langle\bar{i}|M_\nu^\dagger M_\mu|\bar{j}\rangle = C_{\nu\mu}\delta_{ij}}$. Used that $\sum_i |c_i|^2 = 1$.

Example: Shor's code and one weight Pauli errors

$$|0\rangle \to |\bar{0}\rangle = \frac{1}{2^{3/2}}(|000\rangle + |111\rangle)(|000\rangle + |111\rangle)(|000\rangle + |111\rangle)$$
$$|1\rangle \to |\bar{1}\rangle = \frac{1}{2^{3/2}}(|000\rangle - |111\rangle)(|000\rangle - |111\rangle)(|000\rangle - |111\rangle)$$

$\langle \bar{j}|P_b P_a|\bar{i}\rangle = C_{ba}\delta_{ij}$ for $P_a, P_b \in \mathcal{E}$

$$\langle \bar{0}|X_a X_b|\bar{0}\rangle = \delta_{ab}$$
$$\langle \bar{1}|X_a X_b|\bar{0}\rangle = 0$$
$$\langle \bar{1}|X_a X_b|\bar{1}\rangle = \delta_{ab}$$

$$\langle \bar{0}|Z_a Z_b|\bar{0}\rangle = \delta_{ab}$$
$$\langle \bar{1}|Z_a Z_b|\bar{0}\rangle = 0$$
$$\langle \bar{1}|Z_a Z_b|\bar{1}\rangle = \delta_{ab}$$

- Same holds for Y_a operators
- But, if one of the Paulis is X2*X3

$$\langle \bar{0}|X_1 X_2 X_3|\bar{0}\rangle = 1$$
$$\langle \bar{1}|X_1 X_2 X_3|\bar{0}\rangle = 0$$
$$\langle \bar{1}|X_1 X_2 X_3|\bar{1}\rangle = -1$$

No longer independent of i,j. Thus, X2*X3 cannot be corrected.

Shor's code as stabilizer code

- Pauli group $\mathcal{P}_n = \{\pm 1, \pm i\} \times \{I, X, Y, Z\}^{\otimes n}$
- Stabilizer code subspace is defined by a (stabilizer) subgroup $\mathcal{S} \subset \mathcal{P}_n$ as the vector subspace that is fixed by all the elements in $\mathcal{S} \subset \mathcal{P}_n$

$$\boxed{\mathcal{C} = \{|\psi\rangle \in \mathcal{H} \big| S|\psi\rangle = |\psi\rangle \, \forall S \in \mathcal{S}\}}$$

Joint +1 eigenspace of set of commuting Pauli strings

  - Stabilizer group must not contain (-I) and it is Abelian
  - Sufficient to define the codespace via the generators of the stabilizer group only
- For 3-qubit bit flip code: $\mathcal{S} = \langle Z_1 Z_2, Z_1 Z_3 \rangle$
- For Shor's 9-qubit code:

$$\{Z_1Z_2,\ Z_2Z_3,\ Z_4Z_5,\ Z_5Z_6,\ Z_7Z_8,\ Z_8Z_9,\ X_1X_2X_3X_4X_5X_6,\ X_4X_5X_6X_7X_8X_9\}.$$

- Set of logical Pauli gates = set of Pauli operators that commute with all stabilizers = centralizer of $\mathcal{S} \subset \mathcal{P}_n$

Alternatively: $\bar{Z} = X_1X_2X_3 \quad \bar{X} = Z_1Z_4Z_7$

  - Example: $\bar{Z} = X_1X_2X_3X_4X_5X_6X_7X_8X_9$ and $\bar{X} = Z_1Z_2Z_3Z_4Z_5Z_6Z_7Z_8Z_9$

Surface code

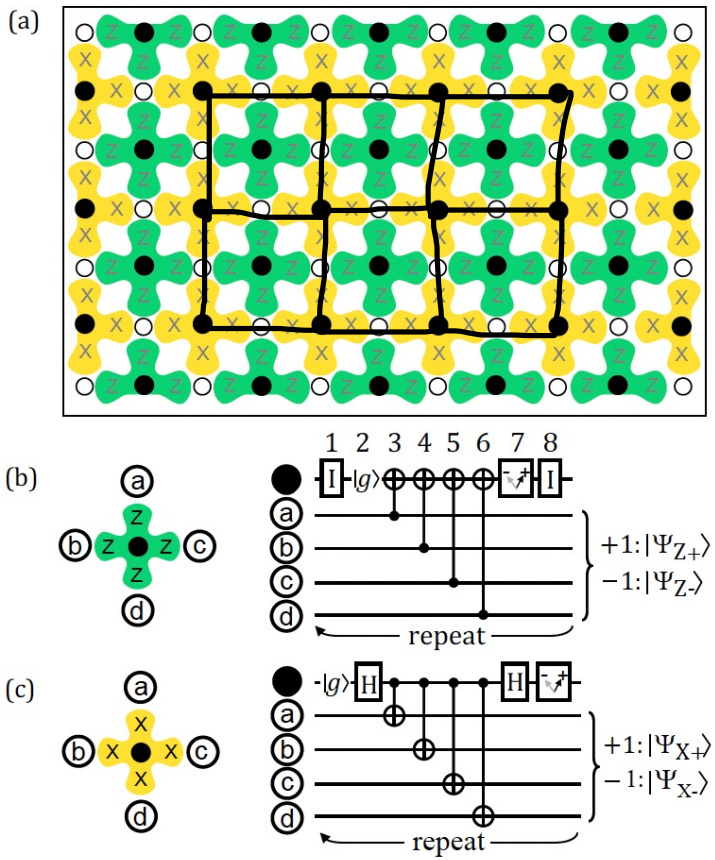

- Planar version of Kitaev's toric code

$$H = -\sum_v A_v - \sum_p B_p$$

$$A_v = \prod_{i \in v} X_i, \; B_p = \prod_{i \in p} Z_i$$

- Data qubits (open circles) on bonds of square lattice
- Local Z and X stabilizers
  - Z checks are product of four Z's around plaquette
  - X checks are product of four X's along star
- GS space is stabilizer space

Kitaev (1997); Dennis et al. (2002); Fowler et al. (2012); Cleland, Sci. Post Lecture Notes (2022)

Logical qubit in surface code

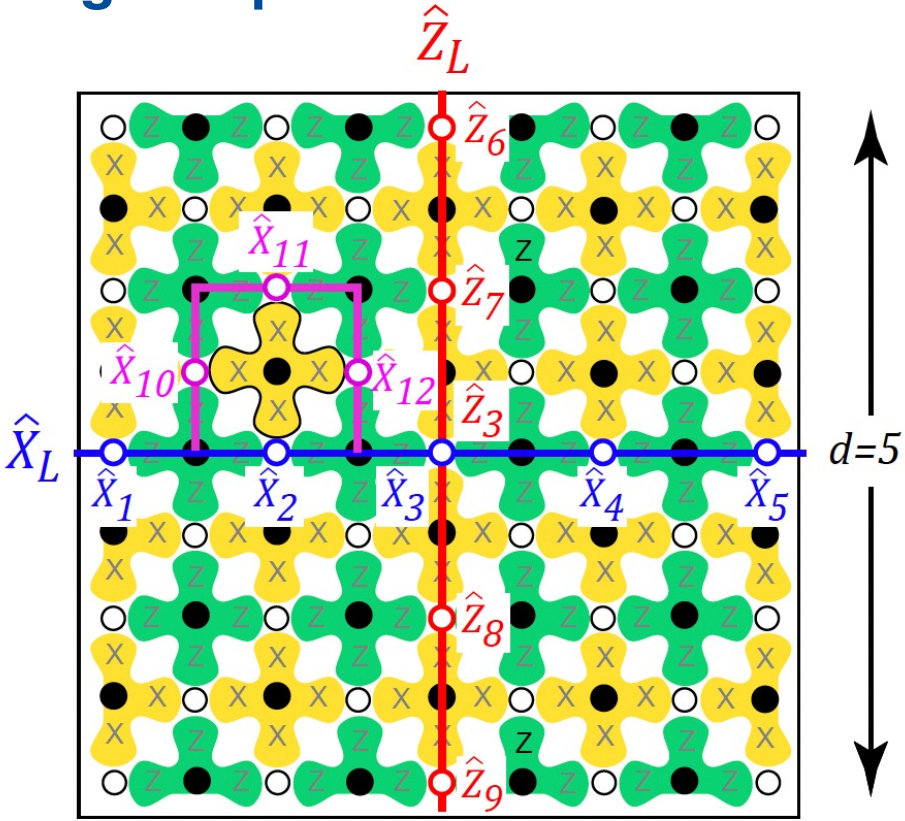

- 41 qubits = 2 x 41 degrees of freedom
- 20 Z and 20 X checks = 2 x 40 constraints
- 2 unconstrained degrees of freedom left = 1 qubit
- State $|\psi\rangle = |u\rangle_L \otimes |v\rangle$ $\in 2^{40}$ dimensional space. Fixed to be a unique state by stabilizer measurements.

Logical qubit

- Logical operators
  - X_L bit flips five qubits, Z_L phase flips five qubits ((change state of array)
  - X_L connects X boundaries, Z_L connects Z boundaries. Here, code distance d = 5.

Fault-tolerant quantum computations

- Compute directly on encoded logical qubits (no decoding necessary)
- Must prevent propagation and accumulation of errors
- Example: logical CNOT for 3-qubit bit flip code

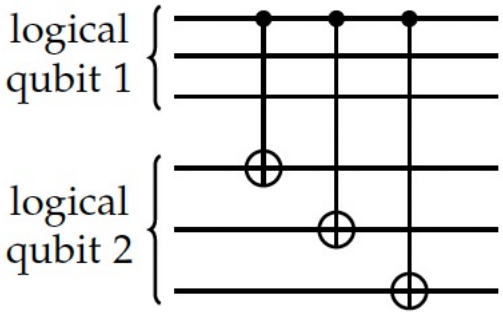

Implementation A

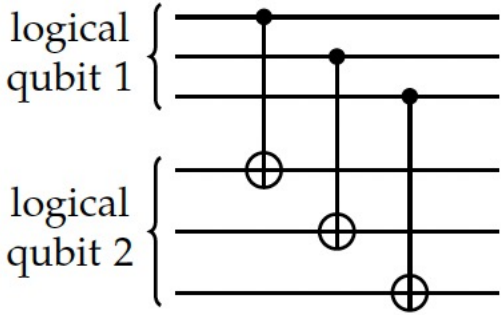

Implementation B

Further reading:

- Nielsen, Chuang, Ch. 10.6
- Cleland, Sci. Post Lecture notes on fault-tolerant gate implementation in surface code

Assume that the only sources of errors are individual controlled-not gates which produce bit-flip errors in their outputs. Which of the two implementations is fault-tolerant?

Summary of Quantum Error Correction part

- Quantum Error Correction protects quantum memory from a chosen set of correctable errors
  - Typically chosen as Pauli errors below some weight
- Quantum information is encoded nonlocally (locality assumption of the errors)
- Failure probability reduced for sufficient small failure rate of physical qubits
- Different codes exist [[n, k, d]], specified by n = number of physical qubits per block, k = number of logical qubits per block, d = distance determines the maximal weight of errors that can be corrected: $d = 2\,t + 1$
- Examples discussed: bit-flip, phase-flip, Shor code, surface code
- Outlook:
  - Classical codes, CSS codes, stabilizer codes, Qudit codes,
  - Bosonic codes for continuous variable systems
  - Fault-tolerant implementation of universal gate set

Check out:

- arthurpesah.me/blog
- J. Roffe, arXiv:1907.11157
- Nielsen, Chuang, Ch. 10
- Preskill, Lecture Notes, Ch.6
- Rieffel, Polak “Introduction to QC” book

Quantum Computing Applications in Condensed Matter Physics

Focus on near-term applications in pre-fault-tolerant era

Condensed Matter Physics & Materials Science

- Fueled by the many possibilities to combine atoms into (periodic) structures

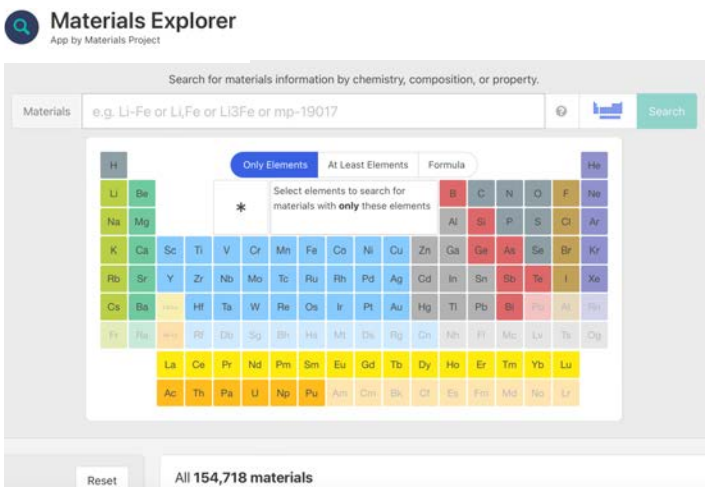

Unconventional superconductors

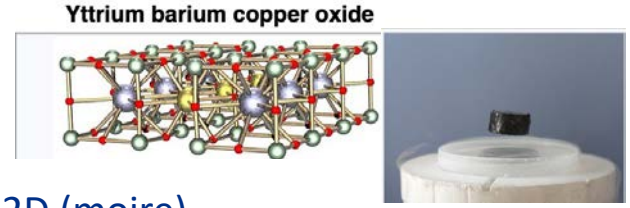

+ emergence due to electronic correlations

2D (moire) materials

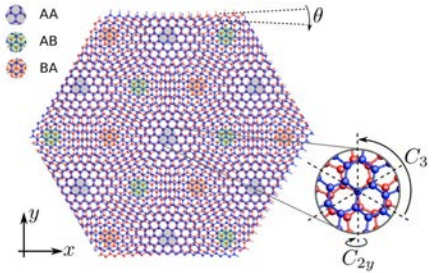

Exotic magnets

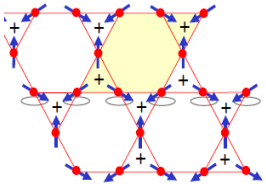

- Goal: Understand & predict quantum materials' properties
  - Equilibrium behavior: phase diagrams, response functions at T=0 and T>0
  - Nonequilibrium behavior: driven systems, quenches, metastable states, kinetic pathways

Common theoretical approach: separation of scales

- Workflow of building realistic effective models for solids
  - Start with atomistic description (theory of everything)

$$
\begin{aligned}
H' &= T_e + V_{ee} + T_i + V_{ii} + V_{ei} + H_{so} + H_{hyper} + H_{rel} + H_{ext} \\
T_e + V_{ee} &= -\sum_j \frac{\hbar^2}{2m_e}\nabla_j^2 + \frac{1}{2}\sum_{j\neq k}\frac{e^2}{|r_j - r_k|} \\
T_i + V_{ii} &= -\sum_J \frac{\hbar^2}{2M_J}\nabla_J^2 + \frac{1}{2}\sum_{J\neq K}\frac{Z_J Z_K e^2}{|R_J - R_K|} \\
V_{ei} &= -\sum_{j,J}\frac{Z_J e^2}{|r_j - R_J|},
\end{aligned}
$$

- so: spin-orbit coupling
- hyper: hyperfine coupling
- rel: relativistic corrections
- ext: external fields

Neglect of simplicity on following slides, but can be quite important, e.g. in topological materials

Common theoretical approach: separation of scales

- Workflow of building realistic effective models for solids
  - Start with atomistic description (theory of everything) ➢ Born-Oppenheimer approximation ➢ treat Coulomb interactions approximately, e.g. within Density Functional Theory (DFT)

$$[T_e + V_{ee} + T_i + V_{ii} + V_{ei}]\Phi(\mathbf{r},\mathbf{R}) = E^{tot} \cdot \Phi(\mathbf{r},\mathbf{R})$$

$$\Phi(\mathbf{r},\mathbf{R}) \cong \Psi_n(\mathbf{r};\mathbf{R})\chi_{np}(\mathbf{R})$$

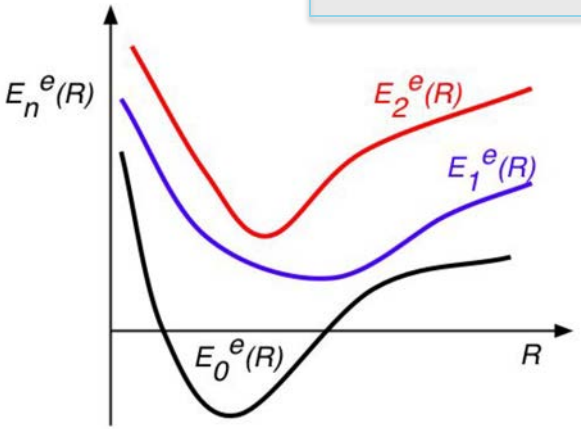

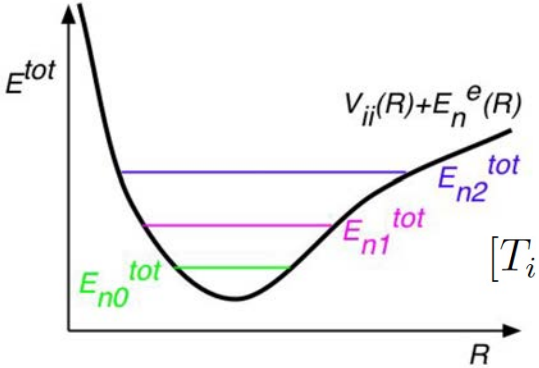

Oppenheimer, c. 1944

$$[T_i + V_{ii} + E_n^e(\mathbf{R})]\chi_{np}(\mathbf{R}) = E_{np}^{tot} \cdot \chi_{np}(\mathbf{R})$$

$$[T_e + V_{ee} + V_{ei}]\Psi_n(\mathbf{r};\mathbf{R}) = E_n^e(\mathbf{R}) \cdot \Psi_n(\mathbf{r};\mathbf{R})$$

Downfolding to most important electronic orbitals

- Workflow of building realistic effective models for solids
  - Start with atomistic description (theory of everything) ➢ Born-Oppenheimer approximation ➢ treat Coulomb interactions approximately, e.g. within Density Functional Theory (DFT)
  - Downfold to low-energy states near Fermi surface (e.g. derive electronic Wannier wavefunctions) and build an effective (Hubbard-like) model
  - Effective model treats Coulomb interactions more accurately

Example for illustration: NdNiO2, taken from Been et al, PRX (2021).

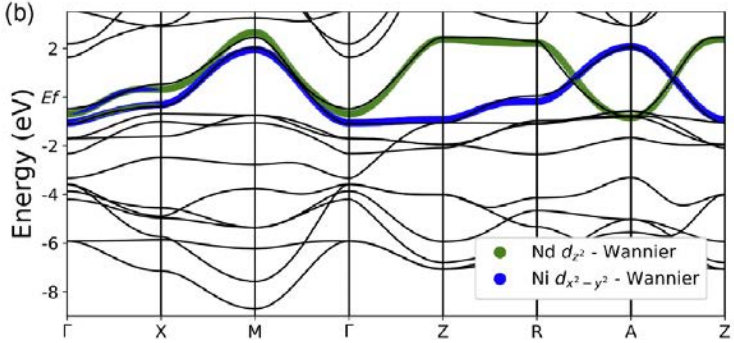

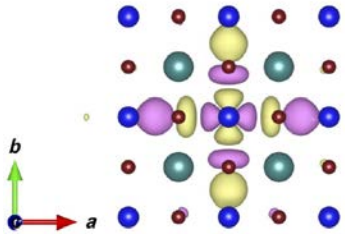

Wannier d_{x2-y2} function

Multiorbital Hubbard model

$$H = \sum_{k,\sigma} (\varepsilon_k^R n_{k,\sigma}^R + \varepsilon_k^{\mathrm{Ni}} n_{k,\sigma}^{\mathrm{Ni}}) + U \sum_i n_{i,\uparrow}^{\mathrm{Ni}} n_{i,\downarrow}^{\mathrm{Ni}} + \sum_{k,i,\sigma} (V_{k,i} c_{k,\sigma}^\dagger d_{i,\sigma} + \mathrm{H.c.}),$$

Effective multiorbital Hubbard-Hund models & spin models

- Workflow of building realistic effective models for solids
  - Start with atomistic description (theory of everything) ➢ Born-Oppenheimer approximation ➢ treat Coulomb interactions approximately, e.g. within Density Functional Theory (DFT)
  - Downfold to low-energy states near Fermi surface (e.g. derive electronic Wannier wavefunctions) and build an effective (Hubbard-like) model
  - Effective model treats Coulomb interactions more accurately
  - Apply further approximations to the model, e.g. derive spin model in strong interaction limit
  - Compute phase diagram and response functions of effective model

Single-band Hubbard model

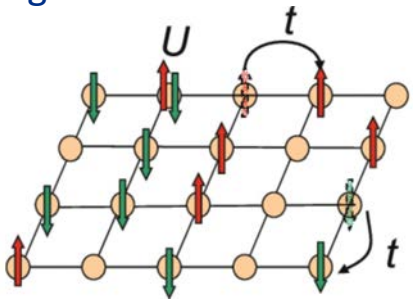

Multiorbital Hubbard model

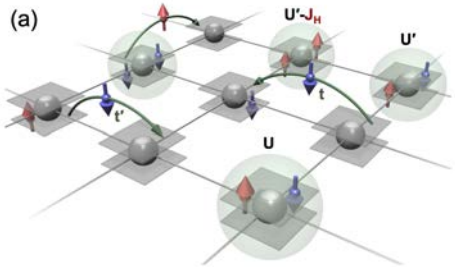

Strong coupling

obtain spin models

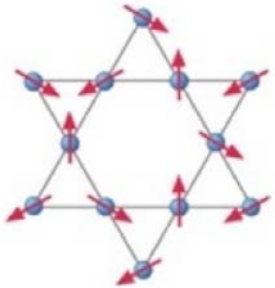

$$H = \sum_{i,j} J_{ij} \mathbf{S}_i \cdot \mathbf{S}_j + \ldots$$

Numerical approaches to effective models

- Solve a small instance of the effective model
  - Exact Diagonalization, Quantum Monte Carlo, Matrix Product States, Tensor Networks, QC
  - Extrapolate to larger systems

Example: Exact diagonalization of spin-1/2 models. Limited to N < 40.

$$|0\rangle = |\downarrow,\downarrow,\downarrow,\ldots,\downarrow\rangle \quad (=0\ldots000)$$
$$|1\rangle = |\uparrow,\downarrow,\downarrow,\ldots,\downarrow\rangle \quad (=0\ldots001)$$
$$|2\rangle = |\downarrow,\uparrow,\downarrow,\ldots,\downarrow\rangle \quad (=0\ldots010)$$
$$|3\rangle = |\uparrow,\uparrow,\downarrow,\ldots,\downarrow\rangle \quad (=0\ldots011)$$

$$H_{ij} = \langle i|H|j\rangle$$
$$i,j = 0,\ldots,2^N-1$$

The Lanczos method

If we need only the ground state and a small number of excitations
- can use "Krylov space" methods, which work for much larger matrices
- basis states with 10^7 states or more can be easily handled (30-40 spins)

The Krylov space and "projecting out" the ground state

Start with an arbitrary state $|\psi\rangle$
- it has an expansion in eigenstates of H; act with a high power Λ of H

$$H^\Lambda|\Psi\rangle = \sum_n c_n E_n^\Lambda |n\rangle = E_0^\Lambda \left(c_0|0\rangle + c_1 \left(\frac{E_1}{E_0}\right)^\Lambda |1\rangle + \ldots \right)$$

For large Λ, if the state with largest $|E_n|$ dominates the sum
- one may have to subtract a constant, *H–C*, to ensure ground state
- even better to use linear combination of states generated for different Λ

$$|\psi_a\rangle = \sum_{m=0}^{\Lambda} \psi_a(m) H^m |\Psi\rangle, \quad a = 0,\ldots,\Lambda$$

- diagonalize H in this basis

From Sandvik, Lecture Notes (2009)

Numerical approaches to effective models

- Embedding Methods
  - Map lattice problem onto impurity model (= small part of the system) coupled to a reservoir (= the rest of the system)
  - Solve self-consistently using ED, QMC, etc to treat the interacting impurity model
  - Becomes exact as the size of the impurity cluster increases

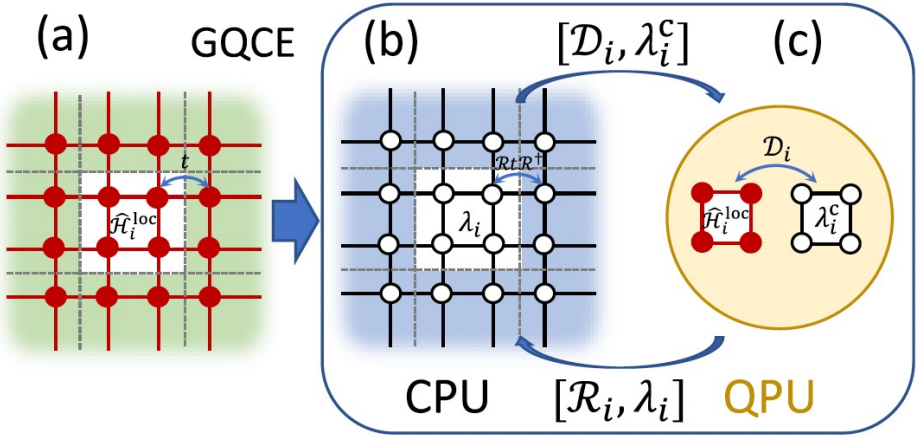

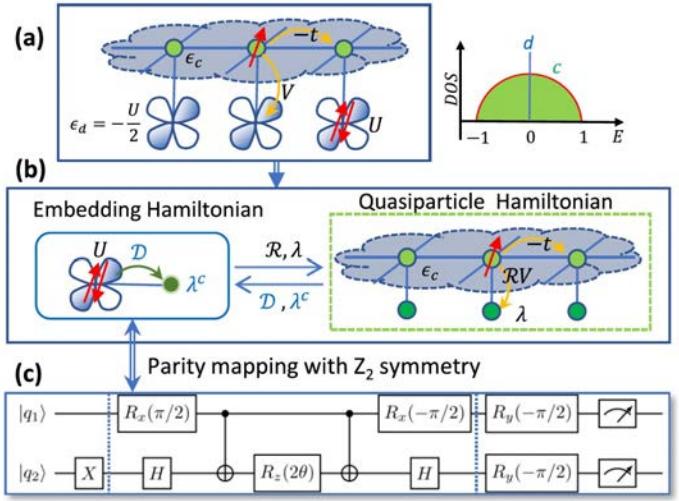

From Yao, …, PPO, PRR (2021).

Opportunities for Quantum Computing

- QC avoids memory bottleneck of classical methods
  - Exponential growth of Hilbert space with system size limits classical methods such as ED
  - Instead: quantum computer can handle exponentially many wavefunction amplitudes (“Nature is not classical”, Feynman)

Opportunities for Quantum Computing

- QC avoids memory bottleneck of classical methods
  - Exponential growth of Hilbert space with system size limits classical methods such as ED
  - Instead: quantum computer can handle exponentially many wavefunction amplitudes (“Nature is not classical”, Feynman)
- QC can deal with highly entangled states
  - Matrix Product States and Tensor Networks are efficient ways to compress a wavefunction
  - The memory requirement is set by the bond dimension that grows as e^S, where S is the entanglement entropy after tracing out part of the system
  - Essentially exact if the wavefunction carries a limited amount of entanglement: constant or logarithmically growing S with system size
  - Breaks down if S grows with system size (volume law)
  - Ground states are often area law entangled (1D gapped states)
  - Excited states generically carry volume law entanglement
    - Relevant at T>0 & in nonequilibrium

Algorithms for Ground State Preparation

- Variational quantum eigensolver (VQE)
- Other notable directions (not covered here)
  - Quantum imaginary time evolution
    - Motta *et al.*, Nature Physics (2020); Ardle *et al.*, (2019)
    - Gomes *et al.*, Adv. Qu. Tech. (2021)
  - Subspace expansion techniques
    - McClean *et al.*, (2017)
    - Bharti *et al.*, Review of Modern Physics (2022).

Variational Quantum Eigensolver

Input

(a) Objective function

$\boldsymbol{\theta} \to \boldsymbol{\theta}_0$

$O\left(\boldsymbol{\theta}, \{\langle H \rangle_{U(\boldsymbol{\theta})}\}\right)$

Output

$\boldsymbol{\theta}^*$

$E_{\text{grd}} \approx O\left(\boldsymbol{\theta}^*\right)$

E_{grd}

distance

$|0\rangle$

$|0\rangle$

$|0\rangle$

$R_z\left(\theta_{1,1}\right)$ $R_x($

$R_z\left(\theta_{2,1}\right)$ $R_x($

$R_z\left(\theta_{3,1}\right)$

$U\left(\boldsymbol{\theta}\right)$

(b) Parametrized quantum circuit

$R_x\left(\pi/2\right)$

I

(c) Basis change

$\min_{\boldsymbol{\theta}} O\left(\boldsymbol{\theta}, \{\langle H \rangle_{U(\boldsymbol{\theta})}\}\right)$

$\boldsymbol{\theta} \to \boldsymbol{\theta}_{\text{new}}$

(d) Classical optimization

Quantum-classical loop

Example from tutorial yesterday (Kagome_gs.ipynb):

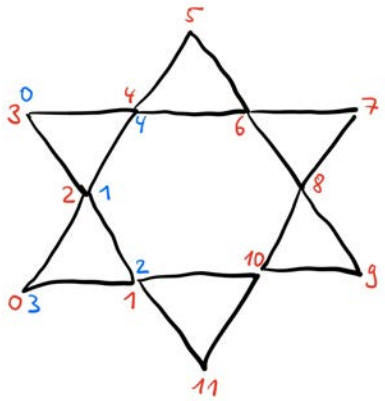

Early work: Peruzzo et al., (2013)

From Bharti et al., RMP (2022)

VQE for Kitaev square-octagon lattice model in magnetic field

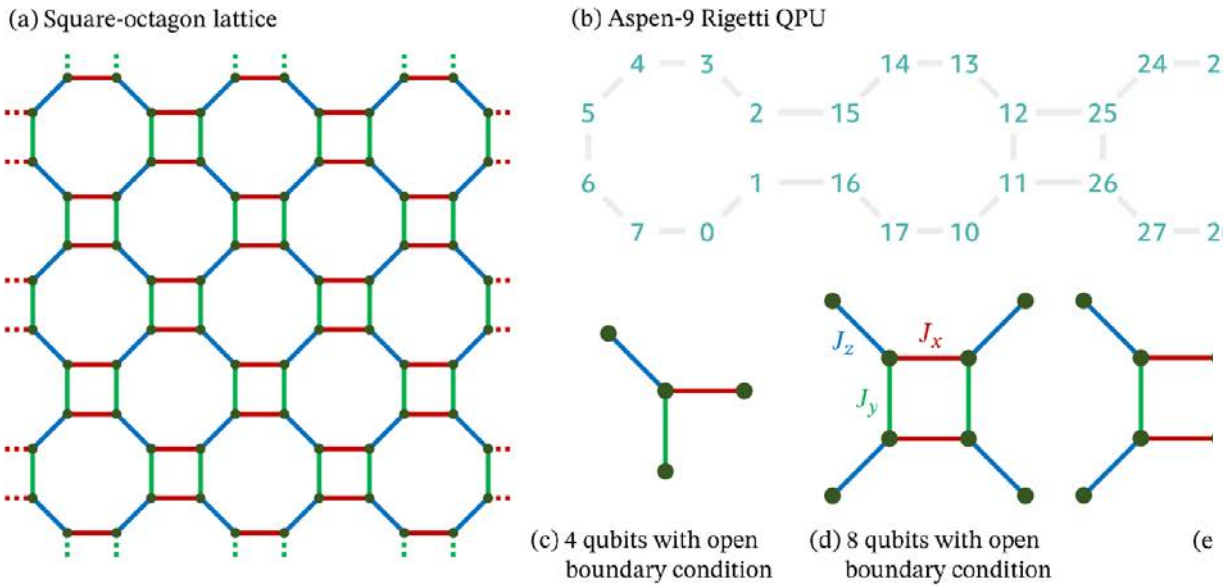

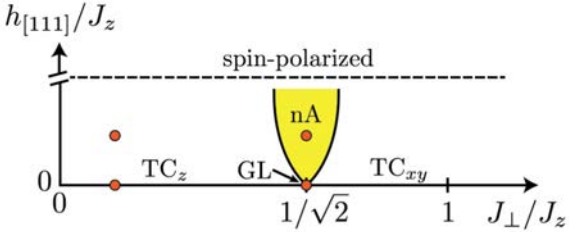

FIG. 2. **Phase Diagram**. Schematic phase diagram of the Kitaev model (2.2) on the square-octagon lattice as a function of spin exchange anisotropy $J_\perp/J_z$ with $J_\perp \equiv J_x = J_y$ and magnetic field in [111] direction $h_{[111]}$. It includes gapped toric code phases (TC_z, TC_{xy}) that are stable with respect to small fields, the gapless line (GL) at $J_\perp/J_z = 1/\sqrt{2}$ and a phase with non-Abelian (nA) Majorana excitations that emerges in field above the gapless line. At large magnetic fields the system enters a spin-polarized paramagnetic phase. The red circles denote the different, representative model parameter points that are studied in our benchmark simulations.

Kitaev model on square-octagon lattice matches Rigetti's QPU geometry. No SWAP gates needed as connectivities match.

From:
Li et al. (SQMS), PRR (2023).

Parametrized quantum circuit (HVA ansatz)

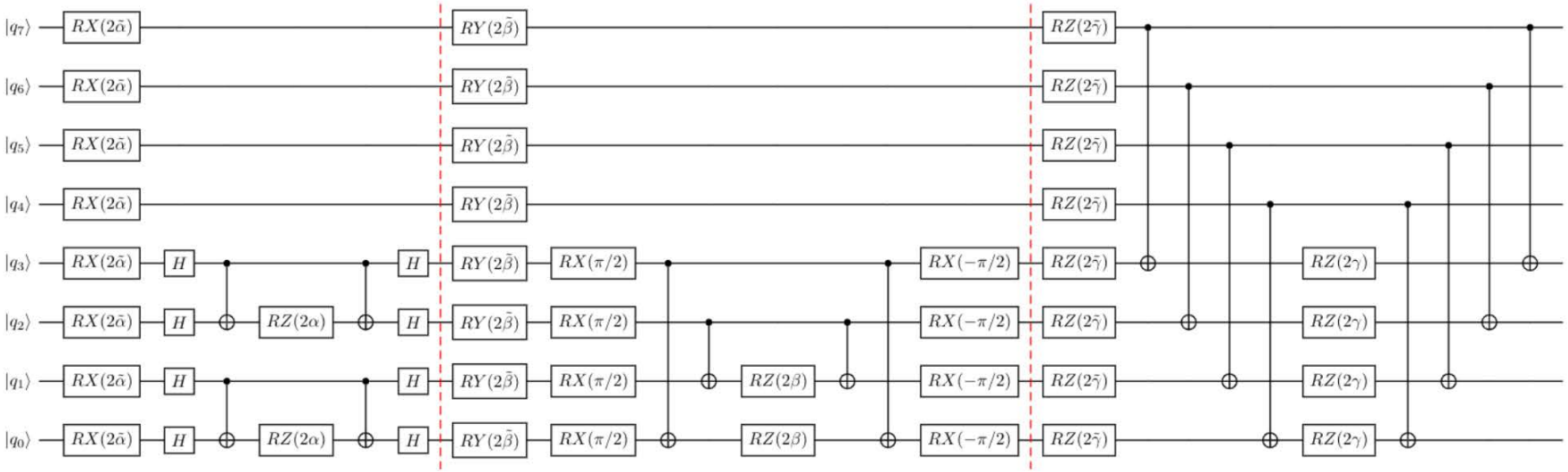

FIG. 3. **HVA with one layer on eight qubits.** The Hamiltonian Variational Ansatz (HVA) with one layer on eight qubits, split into commuting blocks. The first block corresponds to the operation $e^{-i\tilde{\alpha}\sum_q X_q}\ e^{-i\alpha\sum_{(i,j)\in X\text{-links}} X_i X_j}$, the second to $e^{-i\tilde{\beta}\sum_q Y_q}\ e^{-i\beta\sum_{(i,j)\in Y\text{-links}} Y_i Y_j}$, and the third to $e^{-i\tilde{\gamma}\sum_q Z_q}\ e^{-i\gamma\sum_{(i,j)\in Z\text{-links}} Z_i Z_j}$. For the circuit shown here, we used X-links $= \{(q_0,q_1),(q_2,q_3)\}$, Y-links $= \{(q_0,q_3),(q_1,q_2)\}$, and Z-links $= \{(q_0,q_4),(q_1,q_5),(q_2,q_6),(q_3,q_7)\}$.

Statevector and QASM simulations

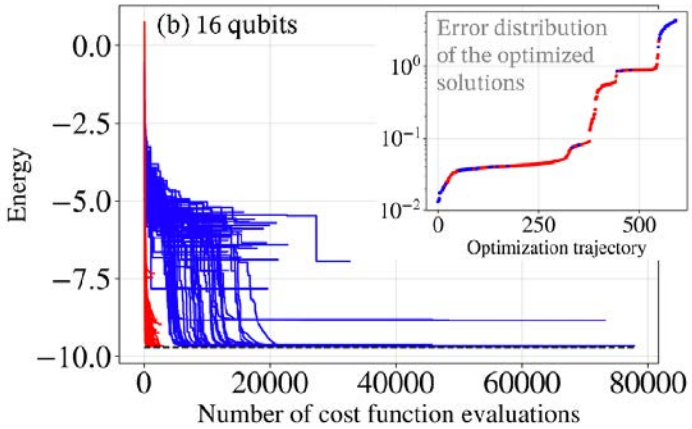

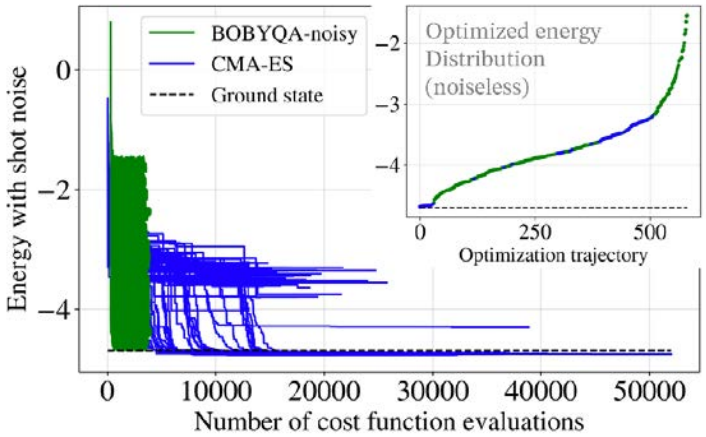

Noiseless: 16 qubits
Noisy: 8 qubits
(8000 shots)

From:
Li et al. (SQMS), PRR (2023).

Conclusions

- Shot noise makes optimization more challenging
- Start from preoptimized solutions for larger systems
- Subspace expansion techniques avoid classical optimization loop (still require many measurements)

Optimizer	Error (noiseless)	Measured deviation	Cost function evaluations
BFGS, 501 initial values	0.45069	0.42052	mean: 747, max: 1994
BOBYQA, 501 initial values	0.27485	0.21843	mean: 471, max: 610
BOBYQA-noisy, 501 initial values	0.07989	-0.00453	mean: 3532, max: 4004
CMA-ES	0.02416	-0.06462	37570
CMA-ES, 80 initial values	0.01610	-0.07125	mean: 21042, max: 52000
Dual annealing	0.04534	-0.01631	60101
SPSA	0.00612	0.00879	100000 (cutoff)

Variational quantum eigensolver for excited states

- Variational quantum eigensolver to prepare highly excited states (VQE-X)
- Minimize energy variance (instead of energy):

$$\mathcal{C}(|\psi(\boldsymbol{\theta})\rangle) = \langle\psi(\boldsymbol{\theta})|H^2|\psi(\boldsymbol{\theta})\rangle - \langle\psi(\boldsymbol{\theta})|H|\psi(\boldsymbol{\theta})\rangle^2$$

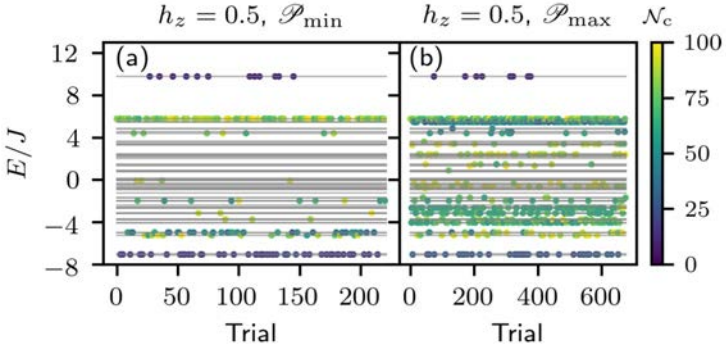

Full coverage of energy spectrum for operator pool with long-range Pauli strings

$$\mathscr{P}_{\max} = \{Y_i\}_{i=1}^N \cup \{Y_iZ_j\}_{i,j=1}^N \cup \{Y_iX_j\}_{i,j=1}^N$$

- Adaptive ansatz construction instead of fixed ansatz
- Nontrivial pool dependence

Zhang, Gomes, Yao, PPO, Iadecola, PRB **104**, 075159 (2021).

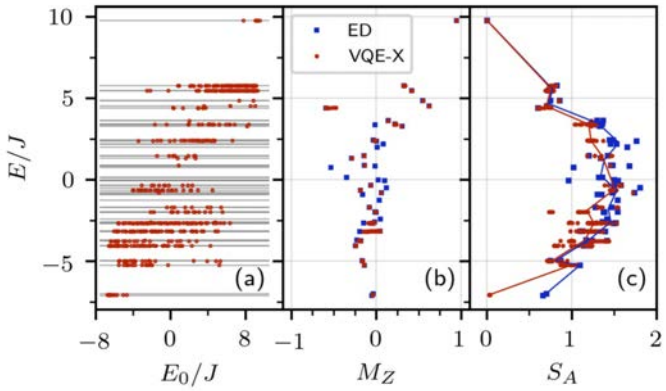

Can investigate properties of volume law highly excited states

Variational quantum eigensolver for excited states

- Variational quantum eigensolver to prepare highly excited states (VQE-X)
- Minimize energy variance (instead of energy):

$$\mathcal{C}(|\psi(\boldsymbol{\theta})\rangle) = \langle\psi(\boldsymbol{\theta})|H^2|\psi(\boldsymbol{\theta})\rangle - \langle\psi(\boldsymbol{\theta})|H|\psi(\boldsymbol{\theta})\rangle^2$$

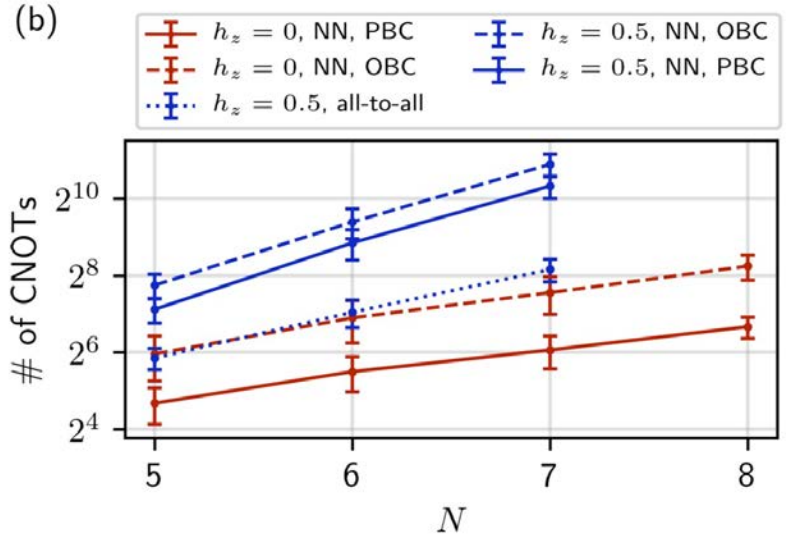

- Exponential scaling of # CNOTs with system size
- Relax convergence condition to represent microcanonical averages instead, see Pollock, PPO, Iadecola, arXiv:2301.04129 (2023).

Zhang, Gomes, Yao, PPO, Iadecola, PRB **104**, 075159 (2021).

Algorithms for Quantum Dynamics Simulations

Applications of real-time dynamics

- Investigate nonequilibrium behavior
  - Chemical reactions
  - Scattering experiments
  - Phase transformations, synthesis, metastable states, kinetic pathways, quenches
  - Fundamental questions: thermalization of a closed quantum system (eigenstate thermalization hypothsis, many-body localization)
  - Scaling behavior in nonequilibrium: transport, nonequilibrium dynamics of order parameters and correlation functions (coarsening, aging)
- Adiabatic state preparation
  - Preparing ground states of Hamiltonians

$$H(t) = H_0(1 - t/T) + H_1 t/T,\ 0 \leq t \leq T$$

Here, we focus on far-from-equilibrium behavior

Quantum dynamics simulations

Initial state

$$|\Psi(0)\rangle = \sum_n c_n |n\rangle$$

Energy eigenstate of many-body H

Dynamics

$$|\Psi(t)\rangle = \sum_n c_n e^{-iE_n t} |n\rangle$$

Dynamics of an observable *O*

$$\langle \mathcal{O}(t)\rangle = \sum_{n,m} c_n c_m^* e^{i(E_m - E_n)t} \langle m|\mathcal{O}|n\rangle$$

$$|\Psi(t)\rangle = \sum_n c_n e^{-iE_n t} |n\rangle$$

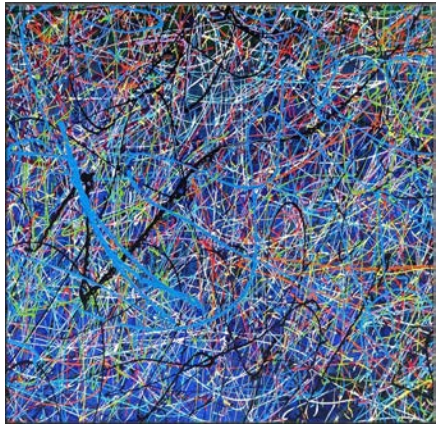

- Classically hard due to rapid growth of entanglement in nonequilibrium for generic H
  - Reason: contains highly excited states ➢ Volume-law entanglement entropy.
  - Need many parameters to classically represent the quantum state
- Quantum simulators and computers can naturally time-evolve a quantum state

Entanglement growth makes classical simulations hard

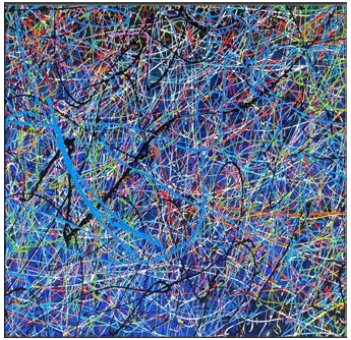

- Time-evolved state $|\Psi(t)\rangle = \sum_n c_n e^{-iE_n t}|n\rangle$ is strongly entangled
- Contains highly excited states of H ➢ Volume-law entanglement

Minimal dimension of matrix product operators (MPO) grows exponentially in time for nonintegrable models (mixed-field Ising model)

Growth is polynomially for integrable models (transverse-field Ising model)

$$H(h^x,h^z) = \sum_{j=0}^{n-2} \sigma_j^x \sigma_{j+1}^x + \sum_{j=0}^{n-1} (h^x \sigma_j^x + h^z \sigma_j^z)$$

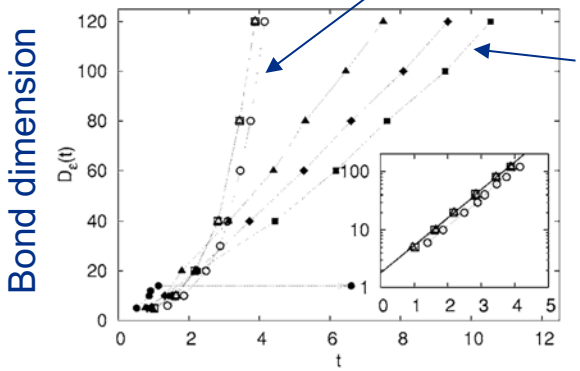

Prosen, Znidaric (2007)

FIG. 3. $D_\epsilon(t)$ for local initial operators. We consider three cases $O(0)=\sigma_{n/2}^{x,y,z}$ (empty circles, squares, and triangles), for nonintegrable evolution H_C, and four cases, $O(0)=\sigma_{n/2}^{x,y}$ (full squares, diamonds), $\sigma_{n/2-1}^z \sigma_{n/2}^y$ (full triangles) with infinite index, and $O(0) = \sigma_{n/2-1}^z \sigma_{n/2}^z$ (full circles) with index 2, for integrable evolution H_R.

Entanglement growth makes classical simulations hard

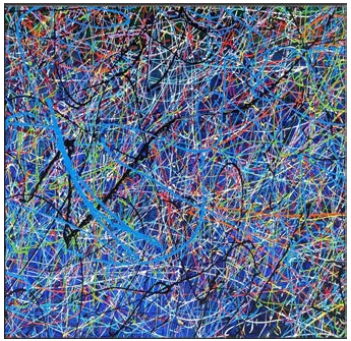

- Time-evolved state $|\Psi(t)\rangle = \sum_n c_n e^{-iE_n t}|n\rangle$ is strongly entangled
- Contains highly excited states of H ➢ Volume-law entanglement

Minimal dimension of matrix product operators (MPO) grows exponentially in time for nonintegrable models (mixed-field Ising model)

Entanglement entropy $S_A = -\mathrm{Tr}[\rho_A \ln \rho_A]$

Reduced density matrix $\rho_A = \mathrm{Tr}_B \rho$

Bond dimension

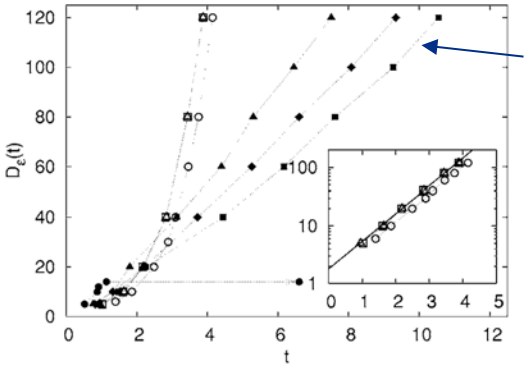

Growth is polynomially for integrable models (transverse-field Ising model)

Prosen, Znidaric (2007)

Entanglement entropy grows ballistically $\propto t$ after global quench

Quench dynamics in Heisenberg model

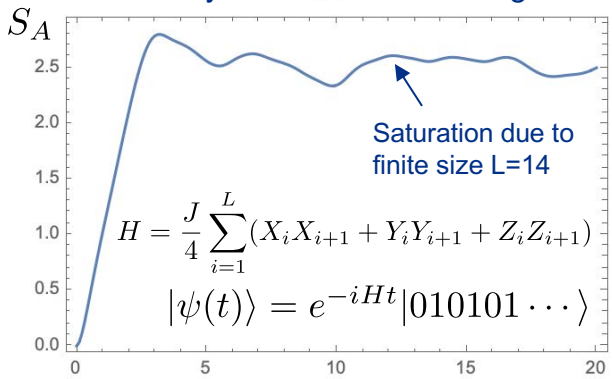

Dynamics simulations are opportunity for quantum advantage

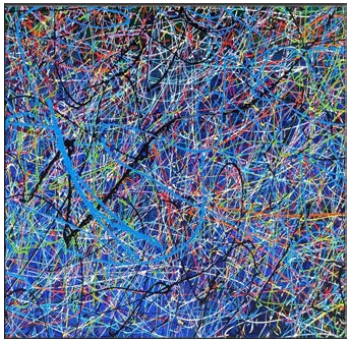

- Time-evolved state $|\Psi(t)\rangle = \sum_n c_n e^{-iE_n t}|n\rangle$ is strongly entangled
- Contains highly excited states of H ➢ Volume-law entanglement

Entanglement = complexity of classical calculation

Exponential growth of classical resources like the bond dimension in tensor networks.
Exact diagonalization is limited by memory.

Opportunity for quantum computing

Bond dimension

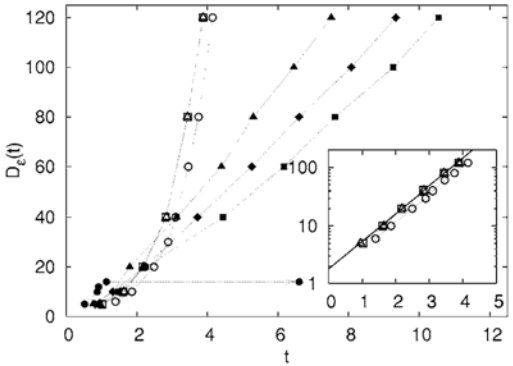

Prosen, Znidaric (2007)

Quench dynamics in Heisenberg model

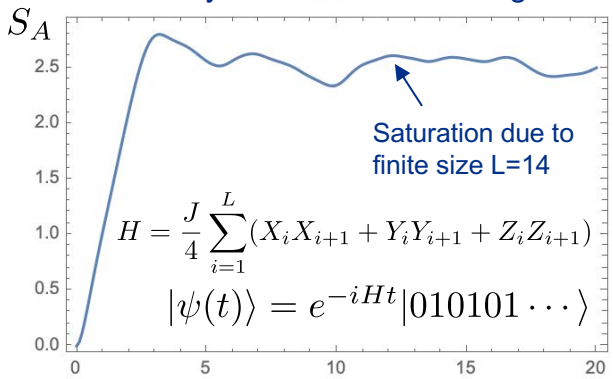

Overview of quantum algorithms for dynamics simulations

$$H = J \sum_i (Z_i Z_{i+1} + h_i Z_i)$$

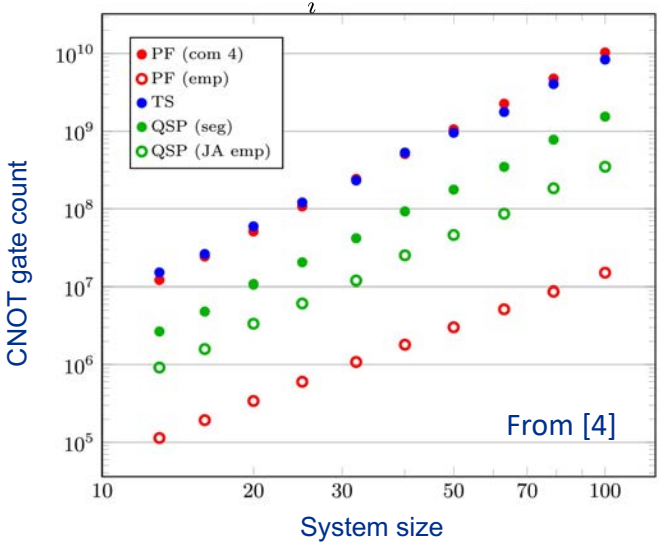

- Lie-Suzuki-Trotter Product formulas (PF)
  - Simple yet limited to early times for current hardware noise
  - Trotter circuit depth scales as $\mathcal{O}(t^{1+1/k})$ ➔ fixed t_f
- Algorithms with best asymptotic scaling have significant overhead
  - Linear combination of unitaries (TS) [1], quantum walk methods [2], quantum signal processing (QSP) [3]
- Hybrid quantum-classical variational methods [5,6]
  - Work with fixed gate depth ☞ ideally tailored for NISQ hardware
  - Trading gate depth for doing many QPU measurements

[1] Berry et al. (2015); [2] Childs (2004); [3] Low, Chuang (2017); [4] Childs et al., PNAS (2018); [5] Li, Benjamin, Endo, Yuan (2019); Y. Yao, PPO, T. Iadecola *et al.* (2021).

Trotter Product Formula approach

- Trotter decomposition of time evolution operator
- Decompose Hamiltonian into sum of terms that include commuting operators
- Example: Mixed-field quantum Ising model

$$H = H_{ZZ} + H_Z + . = V\sum_{i=1}^{L-1} Z_i Z_{i+1} - 2V\sum_{i=2}^{L-1} Z_i - V(Z_1 + Z_L) + \Omega\sum_{i=1}^{L} X_i.$$

Time evolution operator in 1st order Trotter approximation

$$\boxed{U(\Delta t) \approx e^{-iH_{ZZ}\Delta t} e^{-iH_Z \Delta t} e^{-iH_X \Delta t}}$$

$$R_X(\theta_i^X) = e^{-i\theta_i^X X_i/2}$$

$$R_Z(\theta_i^Z) = e^{-i\theta_i^Z Z_i/2}$$

$$R_{ZZ}(\theta_i^{ZZ}) = e^{-i\theta_i^{ZZ} Z_i Z_{i+1}/2}$$

Standard decomposition of RZZ into CNOT and RZ

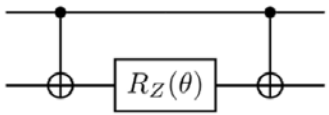

One step of Trotter circuit in L=5 system, starting in Neel state.

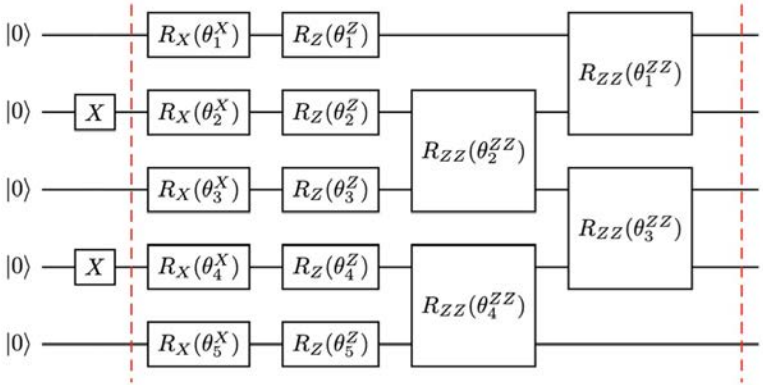

NISQ Trotter simulations of mixed field Ising model

- Benchmark Trotter simulations of mixed-field Ising model on current NISQ hardware

$$H = H_{ZZ} + H_Z + H_X = V\sum_{i=1}^{L-1} Z_i Z_{i+1} - 2V\sum_{i=2}^{L-1} Z_i - V(Z_1 + Z_L) + \Omega\sum_{i=1}^{L} X_i.$$

Displays many-body coherent dynamics for $V \gg \Omega$

Bernien, Lukin (2017)

- Naïve Trotter simulation limited to short times due to finite device coherence time

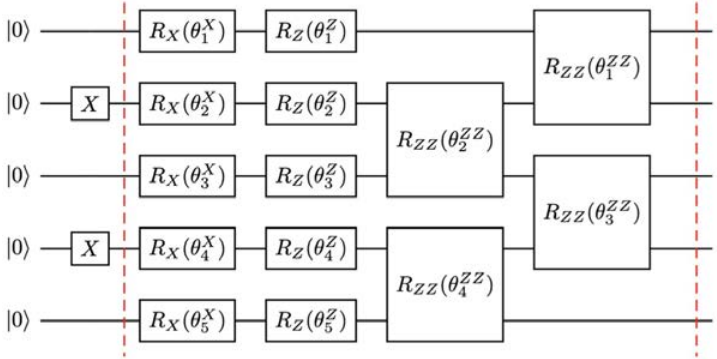

One step of Trotter circuit in L=5 system, starting from Neel state.

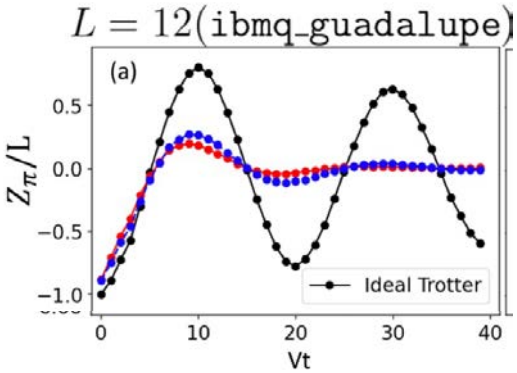

Trotter simulation on QPU ibmq_guadelupe
12 qubits, periodic boundary conditions

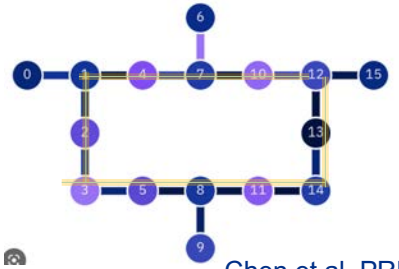

Chen et al, PRR (2022)

Use pulse level control and error mitigation to extend simulation time

Pulse level control and quantum error mitigation (QEM)

- Pulse level control allows to make optimal use of finite coherence time on device
  - Direct implementation of RZZ gate via cross-resonance pulse ➢ cuts program in half
- Quantum error mitigation further extends final time of simulation
  - Readout error mitigation (tensor product assumption): $C_{\text{ideal}} = M^{-1} C_{\text{noisy}}$. $M = \begin{bmatrix} 1-\epsilon_1 & \eta_1 \\ & \eta_1 \end{bmatrix} \otimes \cdots$
  - Zero-noise extrapolation (ZNE) after increasing noise via gate folding $G \mapsto GG^\dagger G$.
  - Pauli twirling: transforming noise to Pauli error channel $\mathcal{N}_\Lambda \rho = \sum_h E_h \rho E_h^\dagger$ $\quad E_h = \sum_{a=0}^{3} \sum_{b=0}^{3} \alpha_{h;a,b} \sigma_c^a \sigma_t^b$
  - Dynamical decoupling: apply $X(\pi)$ and $X(-\pi)$ during qubit idle time
  - Symmetry-based postselection: physically motivated

Pauli twirling

$$\bar{\mathcal{N}}_\Lambda = F_\Lambda[\mathbb{1}] + \sum_{(a,b)\neq(0,0)} \epsilon_{a,b}[\sigma_c^a \sigma_t^b],$$

Postselection into physically relevant part of Hilbert space

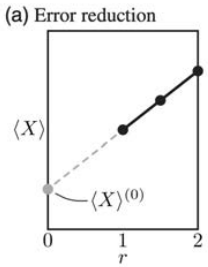

ZNE using mitiq

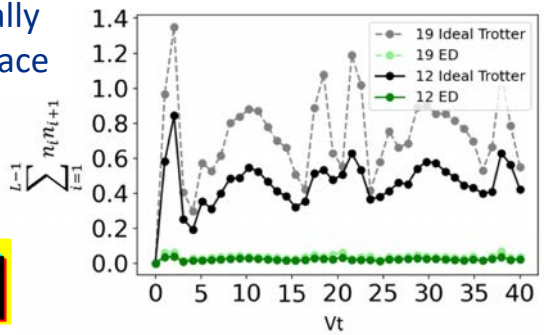

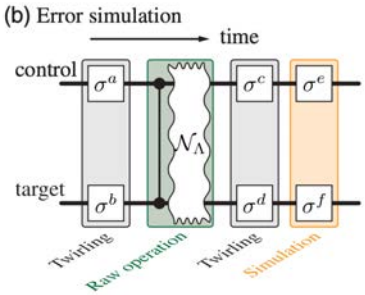

Pauli twirling converts noise to stochastic form ➢ justification for ZNE

Wallmann, Emerson; Li, Benjamin (2017)

Extending simulation time using pulse control and QEM

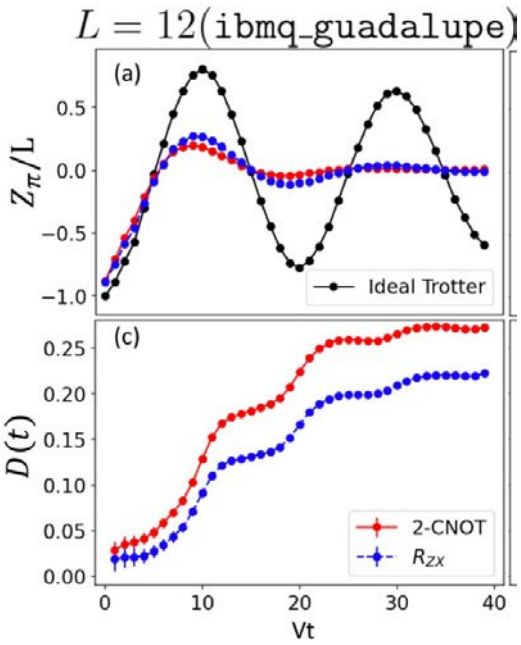

Pulse control

QEM

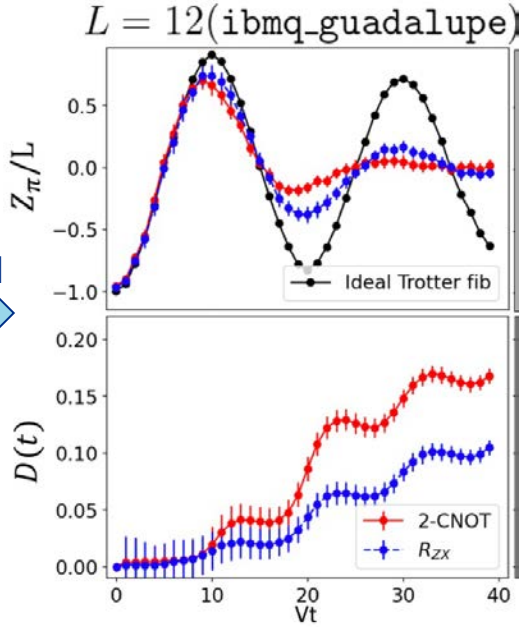

Chen *et al.*, PRR (2022)

Postselection only

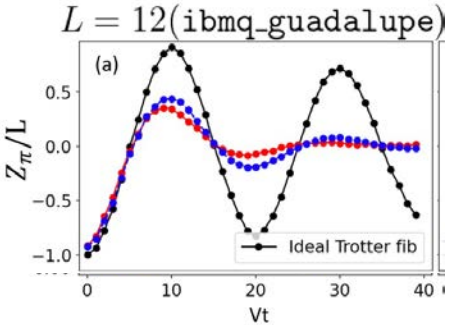

See also the work by the IBM group

Article | Published: 06 February 2023

Scalable error mitigation for noisy quantum circuits produces competitive expectation values

Youngseok Kim, Christopher J. Wood, Theodore J. Yoder, Seth T. Merkel, Jay M. Gambetta, Kristan Temme & Abhinav Kandala

Nature Physics **19**, 752–759 (2023) | Cite this article

Pulse and zero-noise extrapolation (ZNE) are effective strategies to reduce errors.
But: ZNE is heuristic and cannot extend simulation time beyond coherence time of device.

Scaled up simulations: approaching quantum utility regime

- Recent Nature publication from the IBM group: transverse-field Ising model dynamics simulations on 127 qubits
- Uses Zero-Noise Extrapolation (ZNE) informed by sparse Pauli noise tomography

Article | Open Access | Published: 14 June 2023

Evidence for the utility of quantum computing before fault tolerance

Youngseok Kim, Andrew Eddins, Sajant Anand, Ken Xuan Wei, Ewout van den Berg, Sami Rosenblatt, Hasan Nayfeh, Yantao Wu, Michael Zaletel, Kristan Temme & Abhinav Kandala

Nature **618**, 500–505 (2023) | Cite this article

88k Accesses | **6** Citations | **631** Altmetric | Metrics

Hamiltonian

$$H = -J \sum_{\langle i,j \rangle} Z_i Z_j + h \sum_i X_i,$$

Initial state

$$|\psi(t=0)\rangle = |0\rangle^{\otimes 127}$$

- Stimulated several classical simulation works, e.g. Tindall et al., arXiv:2306.14887; Begusic, Chan, arXiv:2306.16372.
- Demonstration of fruitful interplay of quantum and classical simulations

Trotter dynamics of 127 qubit transverse-field Ising model

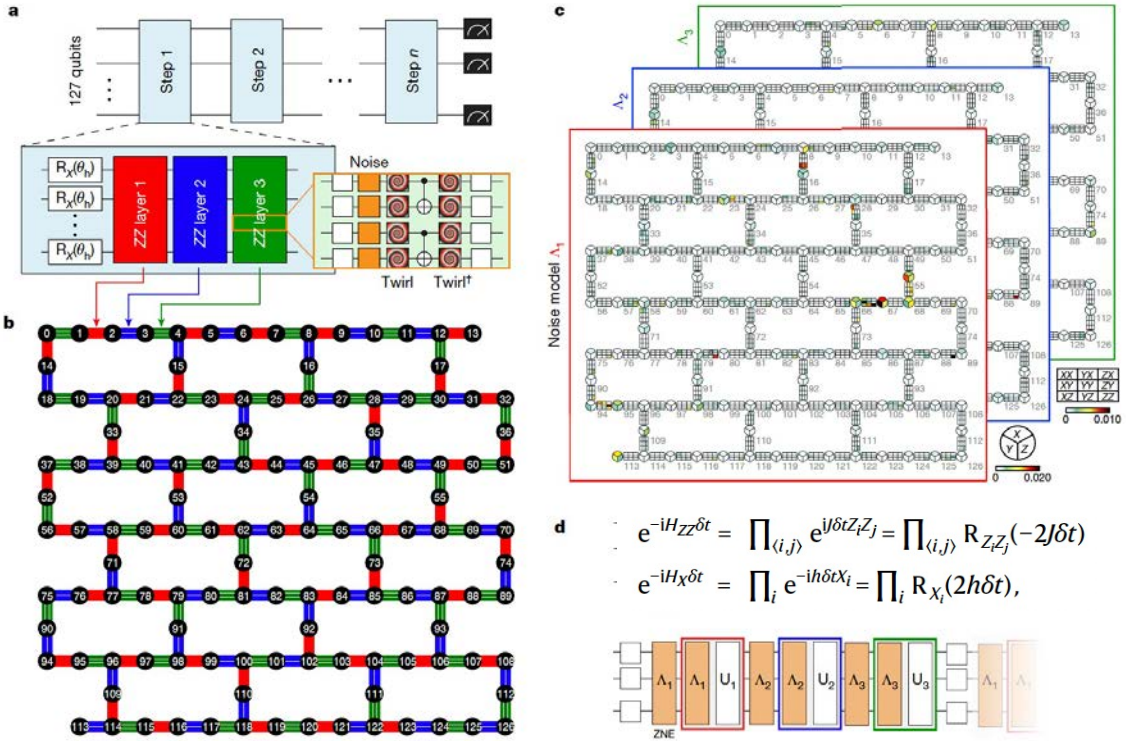

$$e^{-iH_{ZZ}\delta t} = \prod_{\langle i,j\rangle} e^{iJ\delta t Z_i Z_j} = \prod_{\langle i,j\rangle} R_{Z_iZ_j}(-2J\delta t)$$

$$e^{-iH_X\delta t} = \prod_i e^{-ih\delta t X_i} = \prod_i R_{X_i}(2h\delta t),$$

- Trotter circuit contains three layers
- Pauli twirling transforms the noise to Pauli noise
- Efficient noise tomography using a sparse Pauli noise model ansatz
- Can precisely tune the noise for ZNE since noise is well characterized (probabilistic noise amplification)

Trotter dynamics of 127 qubit transverse-field Ising model

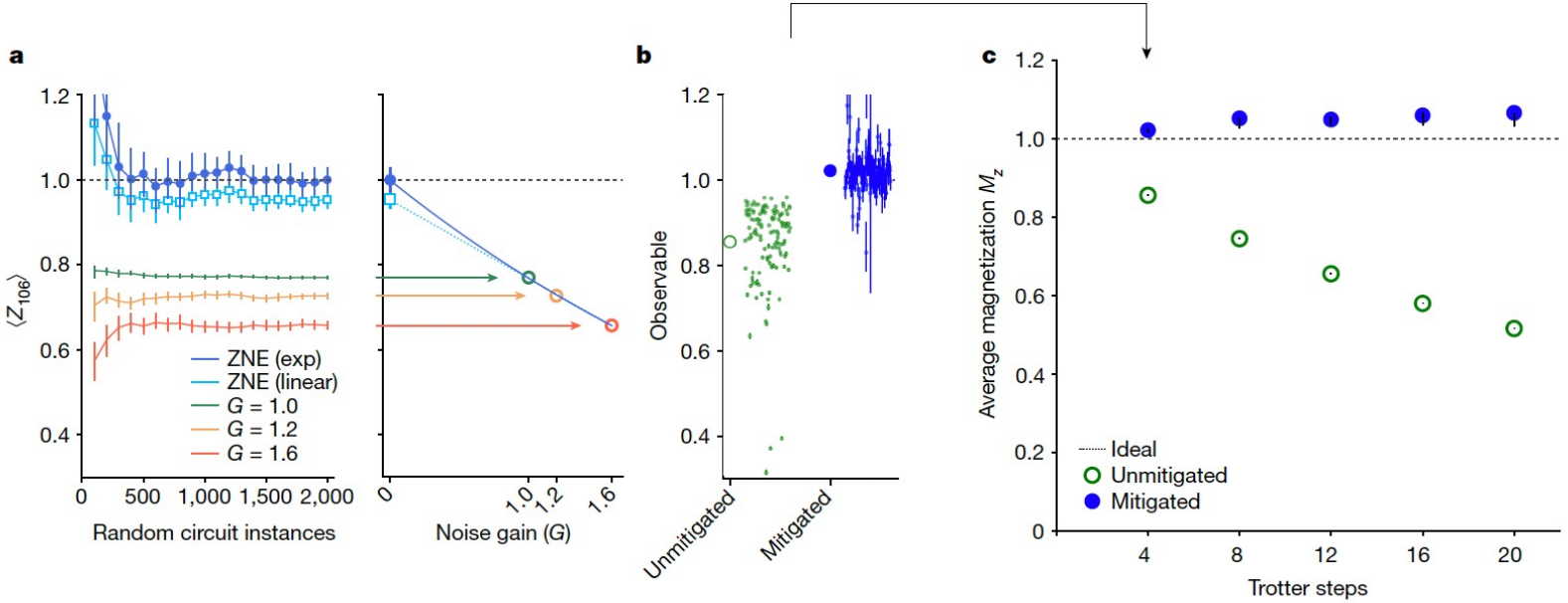

Fig. 2 | Zero-noise extrapolation with probabilistic error amplification. Mitigated expectation values from Trotter circuits at the Clifford condition $\theta_h = 0$. **a**, Convergence of unmitigated ($G = 1$), noise-amplified ($G > 1$) and noise-mitigated (ZNE) estimates of $\langle Z_{106} \rangle$ after four Trotter steps. In all panels, error bars indicate 68% confidence intervals obtained by means of percentile bootstrap. Exponential extrapolation (exp, dark blue) tends to outperform linear extrapolation (linear, light blue) when differences between the converged estimates of $\langle Z_{106} \rangle_{G \neq 0}$ are well resolved. **b**, Magnetization (large markers) is computed as the mean of the individual estimates of $\langle Z_q \rangle$ for all qubits (small markers). **c**, As circuit depth is increased, unmitigated estimates of M_z decay monotonically from the ideal value of 1. ZNE greatly improves the estimates even after 20 Trotter steps (see Supplementary Information II for ZNE details).

Classically verifiable regime

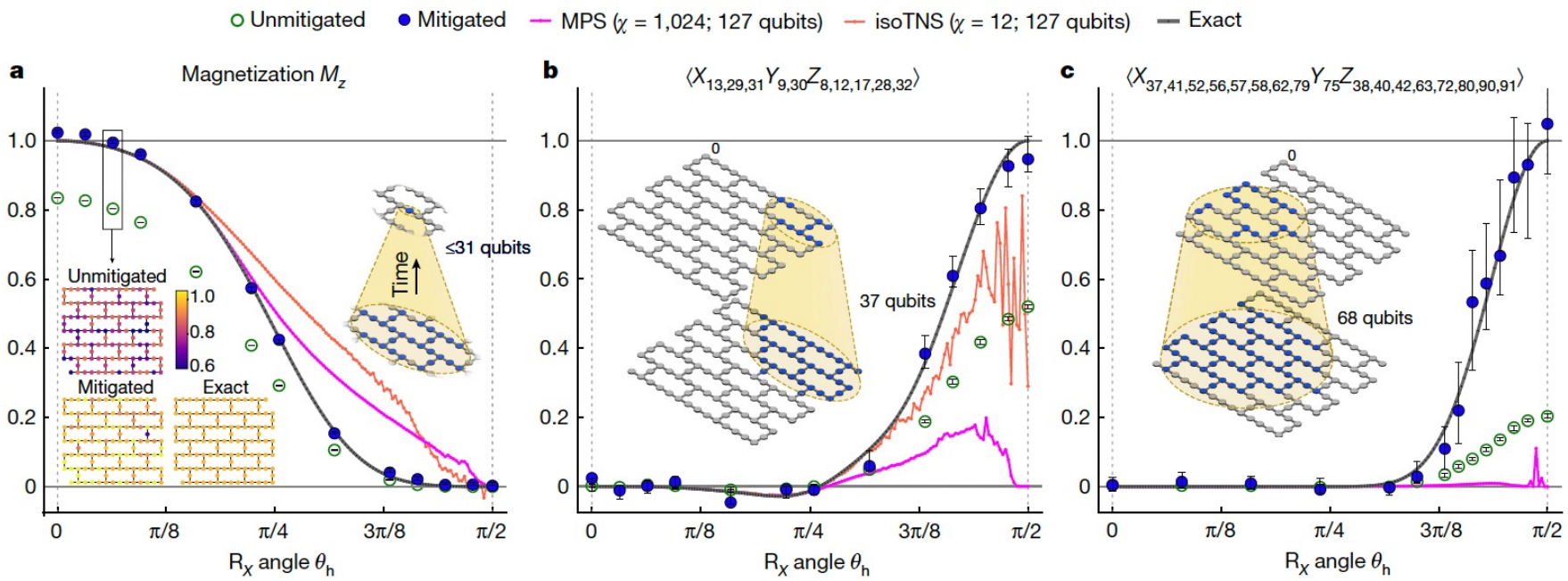

Fig. 3 | Classically verifiable expectation values from 127-qubit, depth-15 Clifford and non-Clifford circuits. Expectation value estimates for θ_h sweeps

Upper insets in all panels illustrate causal light cones, indicating in blue the final qubits measured (top) and the nominal set of initial qubits that can

Classically "challenging" regime

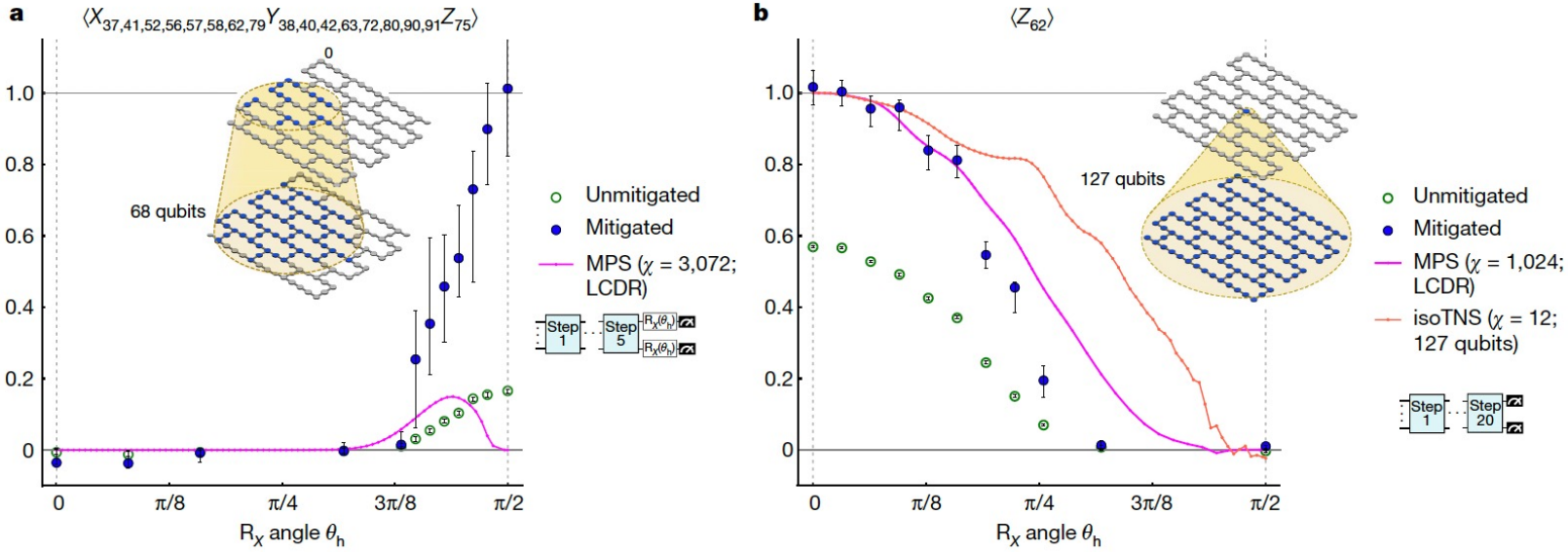

Fig. 4 | Estimating expectation values beyond exact verification. Plot

Even if this work is not yet beyond classical capabilities, it is clear that Trotter dynamics is a leading candidate for quantum advantage

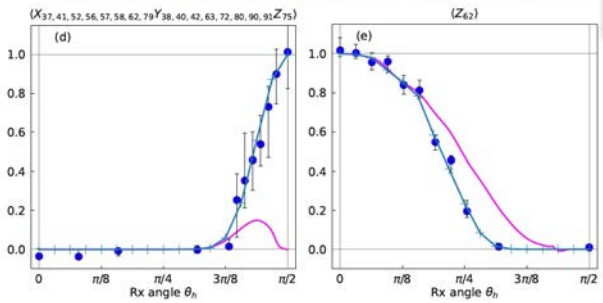

Classical simulations using sparse Pauli dynamics method (Begusic, Chan, arXiv (2023).

Variational Quantum Dynamics

Variational form of quantum state

$$|\Psi[\boldsymbol{\theta}]\rangle = \prod_{\mu=0}^{N_{\boldsymbol{\theta}}-1} e^{-i\theta_\mu \hat{\mathcal{A}}_\mu} |\Psi_0\rangle$$

Variational parameters evolve in time

Von Neumann equation

$$\frac{d\rho}{dt} = \mathcal{L}(\rho) = -i[\mathcal{H}, \rho]$$

$$L^2 \equiv \left\| \sum_\mu \frac{\partial \rho[\boldsymbol{\theta}]}{\partial \theta_\mu} \dot{\theta}_\mu - \mathcal{L}[\rho] \right\|^2$$

$$= \sum_{\mu\nu} M_{\mu\nu} \dot{\theta}_\mu \dot{\theta}_\nu - 2 \sum_\mu V_\mu \dot{\theta}_\mu + \mathrm{Tr}\left[\mathcal{L}[\rho]^2\right].$$

MacLachlan distance b/w exact and variational time evolution

[1] Li, Benjamin, Endo, Yuan (2019).

Variational Quantum Dynamics

Variational form of quantum state

$$|\Psi[\boldsymbol{\theta}]\rangle = \prod_{\mu=0}^{N_{\boldsymbol{\theta}}-1} e^{-i\theta_\mu \hat{\mathcal{A}}_\mu} |\Psi_0\rangle$$

Variational parameters evolve in time

Von Neumann equation

$$\frac{d\rho}{dt} = \mathcal{L}(\rho) = -i[\mathcal{H}, \rho]$$

$$L^2 \equiv \left\| \sum_\mu \frac{\partial \rho[\boldsymbol{\theta}]}{\partial \theta_\mu} \dot{\theta}_\mu - \mathcal{L}[\rho] \right\|^2$$

$$= \sum_{\mu\nu} M_{\mu\nu} \dot{\theta}_\mu \dot{\theta}_\nu - 2 \sum_\mu V_\mu \dot{\theta}_\mu + \mathrm{Tr}\left[\mathcal{L}[\rho]^2\right].$$

MacLachlan distance b/w exact and variational time evolution

Minimize L^2

M measures state change under parameter change

$$M_{\mu\nu} \equiv \mathrm{Tr}\left[\frac{\partial \rho[\boldsymbol{\theta}]}{\partial \theta_\mu} \frac{\partial \rho[\boldsymbol{\theta}]}{\partial \theta_\nu}\right]$$

$$V_\mu \equiv \mathrm{Tr}\left[\frac{\partial \rho[\boldsymbol{\theta}]}{\partial \theta_\mu} \mathcal{L}[\rho]\right]$$

V depends on Hamiltonian

EOM for variational parameters

$$\boxed{\sum_\nu M_{\mu\nu} \dot{\theta}_\nu = V_\mu.}$$

Matrix $M_{\mu\nu}$ and vector V_μ measured on QPU

Scaling to large system sizes challenging as $N_{meas} \propto N_\theta^2$ and N_θ can grow exponentially with system size for nonintegrable models

☞ Opportunity at early times and for integrable models

[1] Li, Benjamin, Endo, Yuan (2019).

Application: continuous quench in spin chain

- Linear quench of anisotropic XY chain in transverse magnetic field

$$\hat{\mathcal{H}} = -J\sum_{i=0}^{N-2}\left[(1+\gamma)\hat{X}_i\hat{X}_{i+1} + (1-\gamma)\hat{Y}_i\hat{Y}_{i+1}\right] + h_z\sum_{i=0}^{N-1}\hat{Z}_i \quad \text{with} \quad \gamma(t) = 1 - \frac{2t}{T}$$

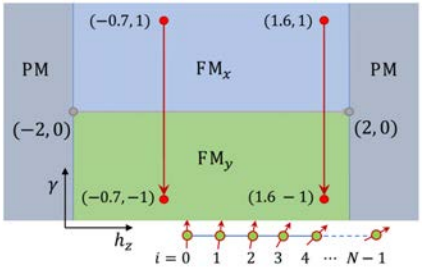

- Follows exact solution during and after quench, shown for N=8
- Circuit depth saturates at 100 CNOTs << Trotter circuit depth $[\![10]\!]$^4 CNOTs
- Simulate system with gate depth independent of time t ➢ can simulate to arbitrary times!

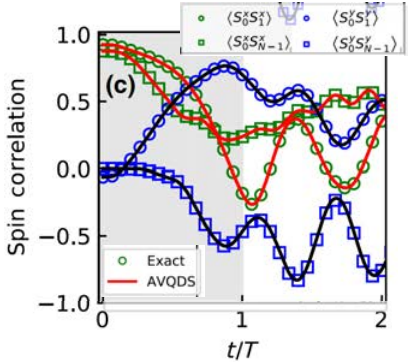

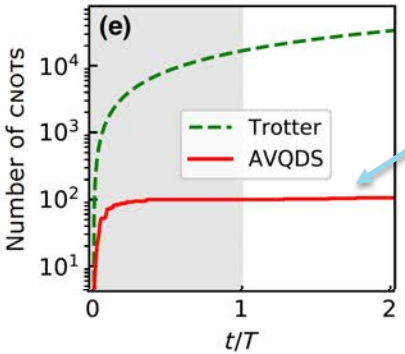

Y. Yao, .., PPO, PRX Quantum (2021)

Summary of CMP applications part

- Condensed Matter Physics provides a rich set of problems that are relevant for domain specialists in physics, chemistry, material science
- Problems are often tunable and thus ideal for benchmarking and tuning into the quantum advantage regime
- Promising directions:
  - Simulation of nonequilibrium quantum dynamics
    - Trotter product formula approach is conceptually simple: combined with quantum error mitigation this is good candidate to reach beyond classical regime soon (maybe already)
    - Multi-product formulas (2207.11268, 2212.14144)
    - Variational methods can in principle extend simulation time further out, but suffer from measurement overhead and difficult classical optimization task
  - Subspace expansion methods avoid classical optimization and are closer in spirit to ED: not covered here, but promising approach both for ground state and dynamics simulations
  - Finite temperature simulations in d > 1: hard classically, so worth trying QC approaches

Thanks for your attention!